Device Characterization of High Performance Quantum Dot Comb Laser

Thesis by

Kazi Ashique Ahmed Rafi

In Partial Fulfillment of the Requirements

For the Degree of

Master of Science

King Abdullah University of Science and Technology

Thuwal, Kingdom of Saudi Arabia

February, 2012

The thesis of Kazi Ashique Ahmed Rafi is approved by the examination committee.

Committee Chairperson: Professor Boon Ooi

Committee Member: Professor Mohammad A. Alsunaidi

Committee Member: Professor Hakan Bagci

ABSTRACT

Device Characterization of High Performance Quantum Dot Comb Laser

Kazi Ashique Ahmed Rafi

The cost effective comb based laser sources are considered to be one of the prominent emitters used in optical communication (OC) and photonic integrated circuits (PIC). With the rising demand for delivering triple-play services (voice, data and video) in FTTH and FTTP-based WDM-PON networks, metropolitan area network (MAN), and short-reach rack-to-rack optical computer communications, a versatile and cost effective WDM transmitter design is required, where several DFB lasers can be replaced by a cost effective broadband comb laser to support on-chip optical signaling. Therefore, high performance quantum dot (Q.Dot) comb lasers need to satisfy several challenges before real system implementations. These challenges include a high uniform broadband gain spectrum from the active layer, small relative intensity noise with lower bit error rate (BER) and better temperature stability.

Thus, such short wavelength comb lasers offering higher bandwidth can be a feasible solution to address these challenges. However, they still require thorough characterization before implementation. In this project, we briefly characterized the novel quantum dot comb laser using duty cycle based electrical injection and temperature variations where we have observed the presence of reduced thermal conductivity in the active layer. This phenomenon is responsible for the degradation of device performance. Hence, different performance trends, such as broadband emission and spectrum stability were studied with

pulse and continuous electrical pumping. The tested comb laser is found to be an attractive solution for several applications but requires further experiments in order to be considered for photonic intergraded circuits and to support next generation computer-communications.

Keywords:

Comb laser, SS-WDM, BBS, LED, SLD, EDFA, PIC, Quantum-Dash, Broadband Laser, Quantum-Dot, Duty cycle, Cavity, LAN, MAN, WDM-PON, BER, Laser, etc.

ACKNOWLEDGEMENTS

I would like to thank my committee chair, Professor Boon Ooi, for his advice and financial support and my committee members, Professor Hakan Bagci and Professor Mohammad A. Alsunaidi, for their guidance and support throughout the course of this research. Also, I would like to thank Dr. Tien Khee who helped with me in conducting some of the experiments and discussing the results. In addition, I would like to thanks all the fellow members of Photonics laboratory for their continuous support.

My appreciation also goes to my colleagues, electrical engineering faculty and staff for making my time at King Abdullah University of Science and Technology (KAUST) a great experience. Moreover, my sincere thanks are extended to my parents for their encouragement and to my friends for their concern and support.

Finally, I would like to thank and dedicate this work to his Majesty King Abdullah Bin Abdulaziz Al-Saud, the custodian of the two holy mosques, for his inauguration and endowment of KAUST.

LIST OF ABBREVIATIONS

AWG	Array Waveguide Gratings
BER	Bit Error Rate
CW	Continuous Wave
CWDM	Coarse Wavelength Division Multiplexing
DWDM	Dense Wavelength Division Multiplexing
DFB Laser	Distributed Feedback Laser
EDFA	Erbium Doped Fiber Amplifier
FWHM	Full Width Half Maximum
FTTH	Fiber To The Home
MAN	Metropolitan Area Network
MLL	Mode Locked Laser
OSNR	Optical Signal-to-Noise Ratio
PON	Passive Optical Network
PIC	Photonic Intergraded Circuits
Rx	Receiver
RT	Room Temperature
SS	Spectrum Sliced / Spectrum Slicing
SMF	Single Mode Fiber
Tx	Transmitter
WDM	Wavelength Division Multiplexing

LIST OF FIGURES

LIST OF TABLES

TABLE OF CONTENTS

CHAPTER 1

INTRODUCTION

1.1 Background

Recent growth in the data and internet transmission technology requires higher bandwidth and longer transmission capacity. Especially, the data networks like metropolitan area network (MAN), passive optical network (PON) require high performance and reliable 1.3-μm semiconductor lasers to meet the excessive demands. Such lasers has been a suitable candidate due to its advanced features like compactness, excitation by electrical injection, wide gain bandwidth, direct modulation, high coherence, high reliability and monolithic integrations [1]. Such emitter is also more reliable over ASE based sources for many integrated devices like OEIC and PIC which been widely deployed in optical communication system, short-reach interconnection in computer systems, measurement, bio-medical and sensing applications. The semiconductor laser can be directly modulated at the microwave frequency range and no external modulators are required since the same current can be used for modulating and biasing [**2**] which is crucial to high speed networks too. As the wavelength division multiplexing (WDM) network in converging to the shorter reaches as LANs, server farms and on chip optical signaling for future energy efficient supercomputers shown in figure 1.1 require cost efficient and reliable emitters.

Further improvement in semiconductor laser performances have been attained due to the precise fabrication of nano-structures such as Quantum- Wells (QW), Quantum-Dots (Q.Dots), Quantum-Dash (Q.Dash) during the crystal growth. In this nano-structured

device, the electrons behavior depends on the quantum nature of the electron and appropriate design of the quantum structure [1].

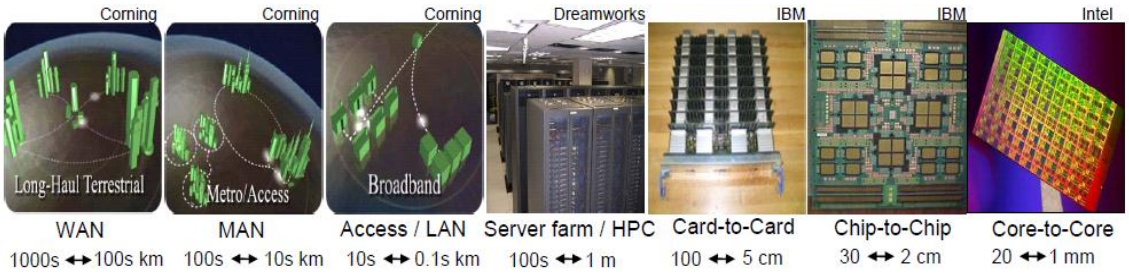

Figure 1.1: The progression of WDM fiber communications which requires economical laser sources to mitigate the future computing and networking demand [3]

Quantum dot lasers have drown consideration attention due to its improved properties liker lower threshold current density, higher thermal stability, higher gain, lower chirp over the bulk / quantum-well semiconductor lasers [4]. Therefore, single multiwavelength quantum-dot comb / mode locked lasers are found to be suitable for short-reach, WDM and computer interconnects as shown in figure 1.2 [3].

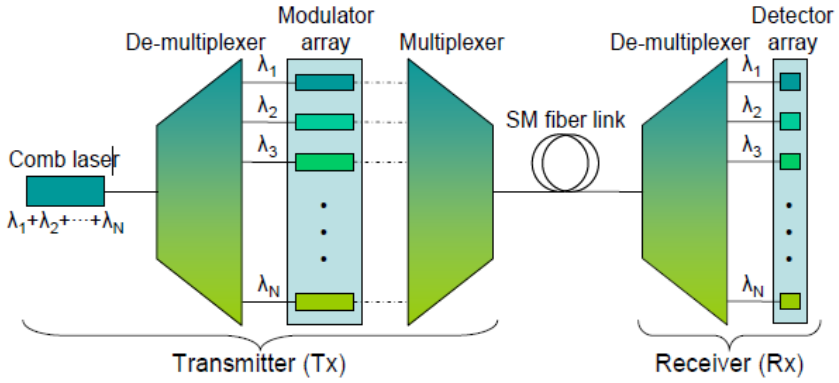

Figure 1.2: Comb transmitter-receiver schematic [3]

These comb lasers are seen as replacement of several DFB lasers used in optical networks. Such devices are also gaining popularity because of the simplicity of operations as no frequency control or external passive devices are required.

1.2 Problem statement

In the recent development of quantum dot mode locked lasers are having several challenges to overcome before its real implementation to the system level. Few of these challenges are addressed as follows [3], [5]:

- It should produce sufficient number of modes / channels with adequate power.
- It should attain broad, flat gain for the desired wavelengths. As an example, it should support O-band and L/C – band which is suitable for WDM applications.
- It should be operating with acceptable threshold current density.
- It should have higher temperature sensitivity.
- Lower relative intensity noise (RIN) level for each of the modes to support the lower bit error rate (BER) high speed applications.

Recently reported quantum dot mode locked laser [5] is very attractive for the direct modulation of individual channels and transmit over the optical fibers. These novel emitters are required to overcome the mentioned challenges before implementing it to WDM-PON, LANs, MANs, and short reach- interconnects. Worth mentioning that during the operations of this mode locked lasers, the injected carrier will raise the temperature causing the external efficiency of the lasers to decrease as well as the wavelength drift. As a consequence, the device modulation performance halts and degrades the general lifetime of laser. Therefore, understanding the degrading factors

and modeling the thermal characteristics of Q.Dot mode locked lasers have become an active research area.

1.3 Scope

Q.Dot lasers suffer performance degradation due to the thermal characteristics of the injection, the lower thermal conductivity of the active layer and due to the additional thermal effects from the resistive heating of the injection [6]. Therefore, further investigations are required to understand the thermal characteristics of the active layers in such QD mode locked lasers. In this project, we will briefly study the performance of the comb laser in conjunction with duty cycle based pumping and by varying external temperature. We will also study the spectrum stability and the wideband gain performance at a controlled injection and as a function of temperature variance. The overall characteristics will be evaluated through the slope and external quantum efficiency which can be found from the light-current (L-I) characteristics of the comb lasers. The three main scopes can be outlined as;

- Observing the performance of Q.Dot mode lock laser with duty cycle variant injection such as pulse, quasi-cw, cw pumping.
- Duty cycle variant injection as a function of temperature variation.
- The bandwidth and spectrum stability with pulse / cw injection.

1.4 Chapter Summary:

The overall thesis has been compiled into six chapters. The related background information, scope, and research gaps have been discussed in this chapter 1. The second chapter consists of mainly 2 parts. In the 1st part, we focused on the conventional

broadband sources such as ASE based sources and their shortcomings. In the 2nd part, we discussed about semiconductor broadband lasers and current state of short wavelength mode locked comb lasers. In this chapter 3, we have briefly discussed the experimental background, scope with the setups used for the characterization of the novel emitter. The experimental finding is conducted in three main streams as duty cycle based characterization, temperature variance characterization and overall spectrum behaviors with pulse / continuous-wave (cw) electrical pumping; has been discussed in chapter 4. For the chapter 5, the overall findings are explained in details from the results and trends found in the previous chapter. Hence, overall conclusion has drawn here with possible recommendations in the final chapter 6.

REFERENCES

[1] Semiconductor Laser Fundamentals Toshiaki Suhara, Osaka University, Japan, CRC Press 2004.
[2] Moustafa Ahmed, Ali El-Lafi, “Large-signal analysis of analog intensity modulation of semiconductor lasers”, Optics & Laser Technology, Volume 40, Issue 6, September 2008.
[3] D. Yin, A. Gubenko, I. Krestnikov et al., “Laser Diode Comb Spectrum Amplification Preserving Low RIN for WDM applications”, Proc. of SPIE, 7631, 76311R(1-7), 2009.
[4] Franois Lelarge; Batrice Dagens; Jeremie Renaudier; R. Brenot; Alain Accard; Frdric van Dijk; Dalila Make; Odile Le Gouezigou; Jean-Guy Provost; Francis Poingt; Jean Landreau; Olivier Drisse; Estelle Derouin; Benjamin Rousseau; Frdric Pommereau; Guang-Hua Duan; , "Recent Advances on InAs/InP Quantum Dash Based Semiconductor Lasers and Optical Amplifiers Operating at 1.55 μm," Selected Topics in -Quantum Electronics, IEEE Journal of , vol.13, no.1, pp.111-124, Jan.-feb. 2007.
[5] Chi-Sen Lee, Wei Guo, Debashish Basu, and Pallab Bhattacharya, “High performance tunnel injection quantum dot comb laser "Appl. Phys. Lett. 96, 101107, 2010.
[6] Hua Tan; Zetian Mi; Bhattacharya, P.; Klotzkin, D.;, "Dependence of Linewidth Enhancement Factor on Duty Cycle in InGaAs–GaAs Quantum-Dot Lasers," Photonics Technology Letters, IEEE , vol.20, no.8, pp.593-595, April15, 2008.

CHAPTER 2

LITERATURE SURVEY

2.1 Comparative Study on Different Conventional Broadband Light Sources

Cost effective optical transceiver system design is becoming very important using efficient light source. It requires the Spectrum Sliced- WDM (SS-WDM) system to meet the high speed demand of the customers and opting for low cost light sources for the progressive WDM networks for several windows in O, S, C, L- band. It started by utilizing the broader emission wavelength of light emitting diode (LED) as a broadband light source. The required wavelength can be used with the aid of different wavelength selective components. The following figure 2.1 shows the spectrum slicing method using AWG or tunable filters that has been used in the past for various short-reach optical interconnects.

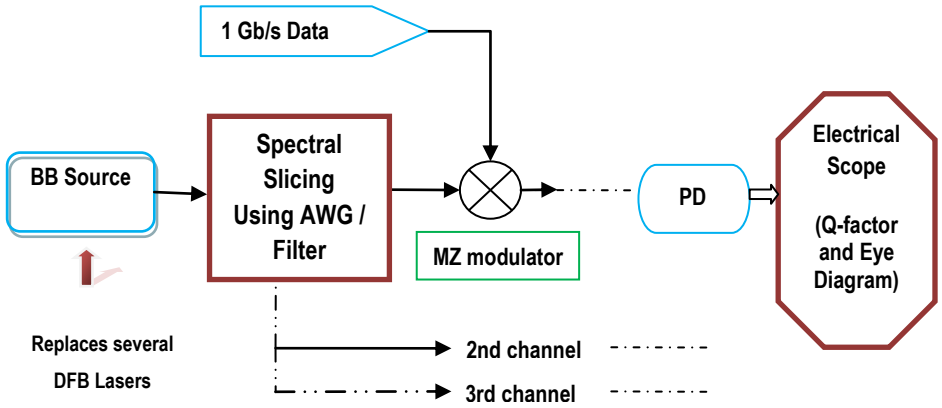

Figure 2.1: Spectrum slicing of typical Broadband Light Sources

SS-WDM utilizing LED also suffers from splicing penalty. From the cost point of view, LED can be cheaper than the laser but it's not fast and power efficient as laser. The output of the LED will fluctuate with time like the thermal noise since spontaneous emission is a dominant factor. 2 Mb/s using LED spectral slicing (SS) for single-mode local loop applications with a power of -25.3 dBm over 2.2 km has been reported by Reeves *et al.* [1]. Recently, 4 channel SS-WDM system using directing modulated 1Gb/s LED has been simulated for a span of 10KM. This approach suffers from extensive losses which would increase substantially if the number of channels are increased and there will be a need of 2 fibers for each bidirectional installation to reduce SNR degradation [2]. Superluminescent diode (SLD) came to the scene, when the need for high power LED is realized for high speed and longer distant optical communication. Moreover, SLD provides simple WDM network provisioning by using spectrum sliced (SS) technique. The 1st demonstrations of broadband-SS transmission using Superluminescent diodes were used to transmit l50 Mbit/s on each of 10 WDM channels, or 50 Mbit/s on each of 16 WDM channels [3]. Later, a WDM system over ll0 km of single mode optical fibre at 140Mbit/s, using a high power superluminescent diode and an erbium fibre amplifier and 9 kilometre transmission without the amplification was reported [4]. A network has been proposed that could accommodate more than 40 subscribers with 622-Mb/s downstream using SS-SLD and 155 Mb/s upstream channels using SS-LED over a single strand of fiber. This proposed network is sensitive to fiber dispersion and requires FEC technique to overcome the limitation of low power LED and extend the transmission distance [5]. 2.5 Gb/s SS-WDM system using optical filters and external modulator was shown in the

paper [6] for short range data communications. This sort of system suffers from excess intensity noise due to incoherent source.

As insufficient power, limited bit-rate operation and operating under short distance are found to be the degrading factors in LED and SLD based SS-WDM system; therefore in 1993, lee et al proposed spectrum slicing of amplified spontaneous emission (ASE) light source of an erbium doped fiber amplifier (EDFA) with various optical bandwidths [7]. Though the power level of EDFA is better than other light sources but it suffers from ASE noise. The ASE noise degrades the system performance by increasing the error floor of BER. The ASE noise can be represented as Gaussian noise whereby it has a flat spectral density over our operating frequency range. The output power in EDFA is defined in equation (2.1) where G is the gain, P_{in} is the input power and P_{ase} is the power of amplified spontaneous emission.

$$P_{out} = G \times P_{in} + P_{ase} \tag{2.1}$$

An Erbium Doped Fiber (EDF) based broadband light source with two output ports has been demonstrated for L and C band for low cost WDM-PON. But this consists of external pump sources and several stages to get the suitable emission wavelength [8]. Following that there are different hybrid methods that have been proposed for low cost WDM system using incoherent broadband sources such as LED and EDFA. The LED has an advantage of direct modulation as well as low fabrication cost, but it cannot support many channels due to its low output power. It also suffers from chirp if it's modulated directly. On the other hand EDFA based spectral slicing method requires expensive external modulation techniques and accompanied with ASE noise. As a result, spectrally

sliced Fabry-Perot (F-P) SLD is proposed but it has a limitation due to intensity noise which has been induced by mode partition and mode fluctuation [9]. This can be mitigated using costly injection locking method [9-10]. Therefore, ASE injected FP semiconductor laser has been demonstrated for error free transmission of 155Mb/s data through 120 km of non-zero dispersion-shifted fiber (NDSF) [11]. DK Jung *et al.* [12] proposed fifteen 500-Mb/s downstream channels and 155-Mb/s upstream channels using a spectrum sliced fiber amplifier light source and fifteen 1550 nm LED's over single strand of conventional SMF which shows a cost effective solution for WDM-PON but may cause crosstalk-induced penalty. This is due to the signal travelling in the opposite direction and signal traversing in the same direction due to the non-ideal shapes of WGR's (Waveguide Grating Router) passband. Moreover, 4-,8- and 16-channel WDM-PON system using broadband ASE source with optical slicing technique has been demonstrated using Optsim software [13]. But with the increment of channel, the system suffers from SNR degradation. Slicing loss and effect on the receiver's sensitivity due to ASE noise addressed as some other drawbacks. ASE based broadband sources have been simulated to demonstrate typical drawbacks as shown in figure 2.2.

To demonstrate ASE based SS-WDM scheme, the broadband laser source spectrum is sliced using either tunable filters or array waveguide gratings (AWG). The conceptual architecture of the novel WDM transmitter is illustrated in Figure 2.1.The feasibility of our design is studied in the following using Rsoft (Optsim and BeamPROP modules).

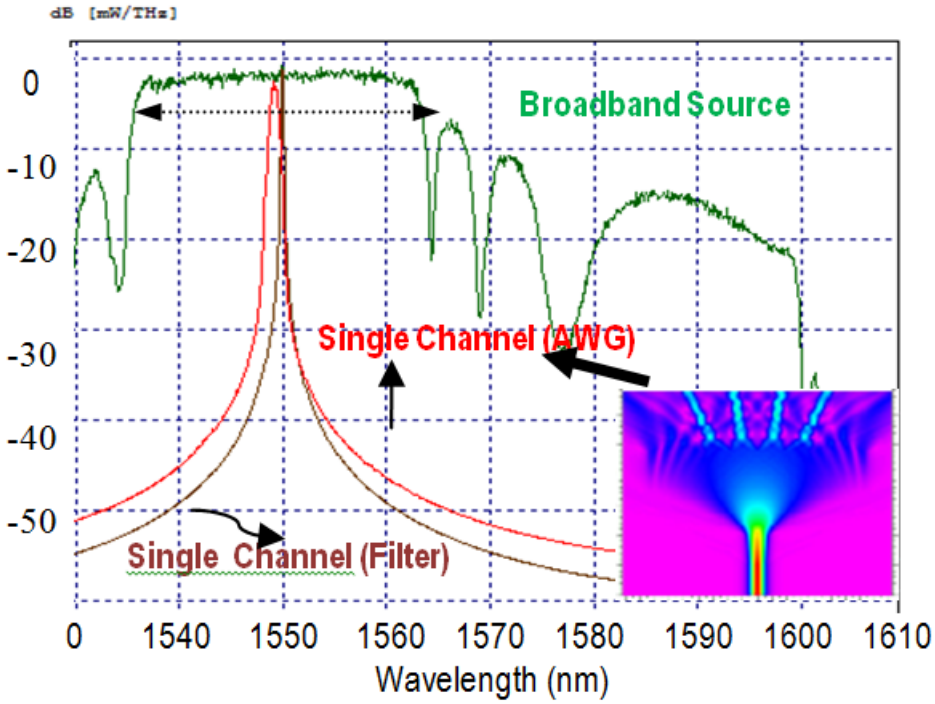

Figure 2.2: the spectrum of ASE BBS spectrum and the extracted single channel spectrum from AWG and filter, respectively (Beam PROP simulated image for AWG spliced BBS is shown in the inset),

The EDFA source has a 10 dB flat gain in conjunction with 30.5 dB ASE noise that gives 25 nm of broadband coverage. High ASE noise embedded in our simulation for achieving a flat emission spectrum. In Figure 2.2, the 1550 nm wavelength is spectrum sliced for 1 Gb/s external amplitude modulation using a filter (brown spectra) and AWG (red spectra) from the broadband source (green spectra). As an example, the BeamPROP simulated image for 1:4 AWG spectrum slicing is illustrated in the inset of Figure 2.2.

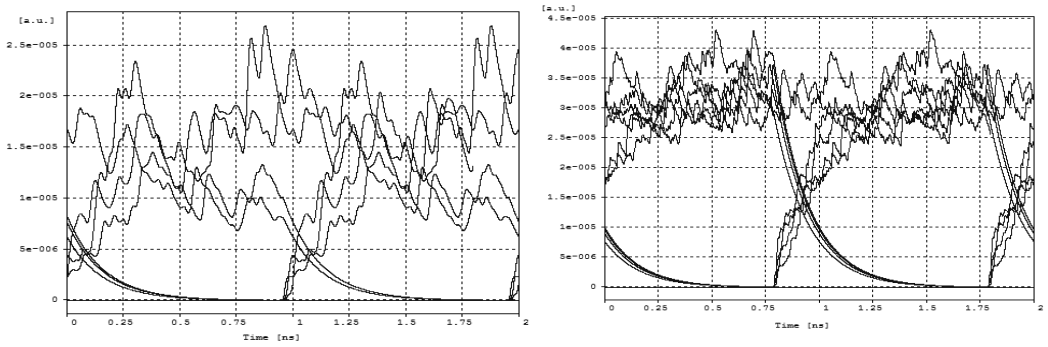

(a) (b)

Figure 2.3: a) Eye diagram for Filter extracted single channel (Q~ 6 dB), b) Eye diagram for AWG extracted channel (Q~23 dB)

The corresponding simulated eye-diagrams are presented in Fig. 2.3(a) and 2.3(b), respectively. Our results show that the Q factors of 6 dB and 23 dB can be obtained using the -2.2 dBm filter-sliced and AWG-sliced ASE BBS, respectively for a low bit rate system.

Although the power penalty values for the filter-sliced and AWG-sliced spectrum are around 13 dBm and 9 dBm, respectively, the simulated Q-factor values do support the bit error rate of $\leq 10^{-9}$ (for $Q \geq 6$) in a short-reach optical communication system. Table 2.1 summarizes the power budget for 1 Gb/s SS-WDM system. Such system is only suitable for low bit rate system and hence suffers from intensity noise, ASE noise and channel crosstalk.

Hence, the typical broadband (BB) sources have several disadvantages which have been summarized in table 2.2. Therefore, broadband semiconductor lasers are found to be the attractive substitute for these conventional broadband light sources and are described in the following section.

Table 2.1: Power budget calculations

	Slicing Techniques	
	Filter	**AWG**
Bit Rate	1 Gb/s	1 Gb/s
Launched Power	-2 to 0 dBm	-2 to 0 dBm
Loss after slicing	-13 dBm	-9 dBm
Loss after modulation	-9 dBm	-6 dBm
Power at the receiver	-22 dBm	-15 dBm
Q-factor	6.02 dB	24 dB

Table 2.2: Cons of different Broadband light sources [14]

Sources	**Cons**
LED	Limited channels, short reach and poor scalability
SLED / SOA	Short distance and low bit rate
EDFA	ASE noise
Injection locked FP	RIN, Distance limited, Non-standard FP required, polarization Dependent
RSOA	Expensive, Seed source required, backscattering, polarization Dependent
REAM	Expensive, Backscattering
Tunable lasers	Expensive, External modulator required, Wavelength assignment algorithm required

REFERENCES

[1] M. H. Reeve, A. R. Hunwicks, W. Zhao, S. G. Methley, L. Bickers, and S. Hornung, “LED spectral slicing for single-mode local loop applications,” Electronics Letters, vol.v24, no. 7, pp. 389-390, Mar. 1988.

[2] I.Ļašuks, A. Ščemeļevs, O. Ozoliņš, "Investigation of Spectrum-sliced WDM System," Electronics and Electrical Engineering. – Kaunas: Tehnologija, No. 5(85). pp. 45–48, 2008.

[3] S. S. Wagner, and T. E. Chapuran, “Broadband high-density WDM transmission using superluminescent diodes,” Electronics Letters, vol. 26, no. 11, pp. 696-697, May. 1990.

[4] P. D. D. Kilkelly, P. J. Chidgey, and G. Hill, “Experimental demonstration of a three channel WDM system over 110 km using superluminescent diodes,” Electronics Letters, vol. 26, no. 20, pp. 1671-1673, Sep. 1990.

[5] K. H. Han, E. S. Son, K. W. Lim, H. Y. Choi, S. P. Jung, and Y. C. Chung, "Bi-directional WDM passive optical network using spectrum-sliced light-emitting diodes," Optical Fiber Communication Conference, paper MF98, Los Angeles , California , USA , Feb. 2004.

[6] M.S. Leeson, B. Luo, and A.J. Robinson, "Spectral Slicing for Data Communications," Proceedings Symposium IEEE/LEOS Benelux Chapter Eindhoven, pp. 165–168, 2006.

[7] J. S. Lee, Y. C. Chung, and D. J. DiGiovanni, “Spectrum-sliced fiber amplifier light source for multichannel WDM applications,” IEEE Photonics Technology Letters, vol. 5, no. 12, pp. 1458-1461, Dec. 1993.

[8] Tae-Won Oh, Jin-Serk Baik, Jae-Ho Song and Chang-Hee Lee, "Broadband Light Source for wavelength -Division Multiple Access Passive Optical Network," OptoElectronics and Communication Conference, Shanghai, China, pp.389-390, 2003.

[9] S. L. Wroodward, P. P. Iannone, K. C. Reichmann, and N. J. Frigo, “A spectrally sliced PON employing Fabry–Perot lasers,” IEEE Photon. Technol. Lett., vol. 10, pp. 1337–1339, Sept. 1998.

[10] K. Petermann, Laser Diode Modulation and Noise. London, U.K.: Kluwer, 1988.

[11] Hyun Deok Kim; Seung-Goo Kang; Chang-Hee Le; , "A low-cost WDM source with an ASE injected Fabry-Perot semiconductor laser," Photonics Technology Letters, IEEE , vol.12, no.8, pp.1067-1069, Aug 2000.

[12] Jung, D.K.; Youn, C.J.; Woo, H.G.; Chung, Y.C.; , "Spectrum-sliced bidirectional WDM PON," Optical Fiber Communication Conference, 2000 , vol.2, no., pp.160-162 vol.2, 2000.

[13] I. Ļašuks, "Investigation of Colorless WDM-PON Using a Broadband ASE-Source," Electroncs and Electrical Engineering ISSN 1392-1215 2009, No.6, Lithuania, Kauņa, 12.-14. pp 43-46, May.2009.

[14] Ning Cheng and Frank Effenberger, "WDM PON: Systems and Technologies", ECOC workshop, Italy. 2010.

2.2 Broadband Emission of Semiconductor Quantum Dash / Dot Laser

In the previous section, we have seen that conventionally amplified spontaneous emission (ASE) based light sources suffers from different drawbacks. Lately, a novel substitute, broadband emission light sources has been found due to the recent advancement of semiconductor lasers. It has drawn attention due to its advanced features like compactness, excitation by injection, wide gain bandwidth, direct modulation, high coherence, high reliability and suitability for monolithic integrations [1] which can be well integrated for WDM, DWDM, WDM-PON, HDWDM, SS-WDM systems. Further improvements in semiconductor laser performances have been attained due to the precise fabrication of the quantum structures during the crystal growth. Optical amplification by stimulated emission in the nano structures like Quantum-Well (QW), Quantum-Dot (Q.Dot), Quantum-Dash (Q.Dash) has converged as area for remarkable scientific research. These lasers will be a suitable candidate for the next generation supercomputing architecture whereby the usages of the on-chip optical signaling is necessary. Furthermore, the applications can be extended to various vital medical applications such as optical coherence tomography (OCT).

During past years, InP / InAs Q.Dash based semiconductor lasers have attracted considerable attention as they operate at the most interesting window for telecommunications (1.4um to 1.6um) as well as for optical fiber communications [2]. Several significant Q.Dot [3] and Q.Dash [4] multi-wavelength wideband emitters have been demonstrated which is seen a perfect replacement of DFB laser arrays shown in fig. 2.4. Broad emission over 50nm was reported from a Q.Dash semiconductor laser in C-band [4] and 75.9 nm from Q.Dot comb laser over O-band [5]. Other unique

characteristics like low threshold current, wide temperature range, feedback insensitivity, low noise, distinctive modulation behavior, excellent phase noise, superior time-jitter characteristics, millimeter wave generation for Radio-On-Fiber (ROF) application have been intensively studied [2,6,7] that makes semiconductor based Q.Dash laser more distinctive candidate for spectrum sliced WDM (SS-WDM) operations. A novel broadband Quantum Dash laser diode for 40-channel WDM transmission has also been demonstrated recently [8]. This is achieved by implementing a laser with a broad lasing linewidth of around 85 nm at 15^{o}C around the L-C optical window. The 40 channel spectral slicing has been done using array waveguide (AWG) kept with the constant of 15^{o}C for stable device operation.

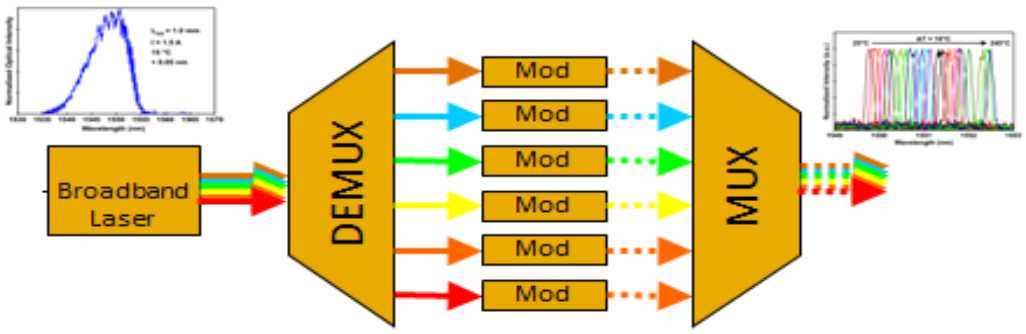

Figure 2.4: Replacement of several DFB lasers with single broadband laser

Furthermore, with the aid of cavity engineering, once the mode spacing is matched to the channel spacing without any aid of frequency control. Therefore, using mode locked lasers (MLL) represents several advantages over the distributed feedback (DFB) laser. Several research works have been done to implement in different optical bands ranging from short to long wavelengths as it can be fully integrated to the WDM transceiver. Surprisingly, interest in comb based mode locked (ML) lasers has also grown interest for

1-µm waveband photonic system due to extensive exploitation in the C- and L-band photonics transport systems as an alternative candidate [9].

Comb generation in an MLL in the C band (1550 nm) using an InP- based quantum-dash (Q.Dash) structure had been successfully reported [10]. The authors in [10] have reported separate error free transmission of 8 channels at 10 Gb/s using a comb based Q.Dot MLL over 50 Km Single mode fiber (SMF) span as shown in figure 2.5. The channel spacing of 100 GHz has been used here and a further efficient comb generation has been reported by Nquyen et al. [11] with 42.5 Ghz channel spacing for emerging WDM-PON set-up [12]. Eventually, other groups have extended the experiment using advanced modulation schemes.

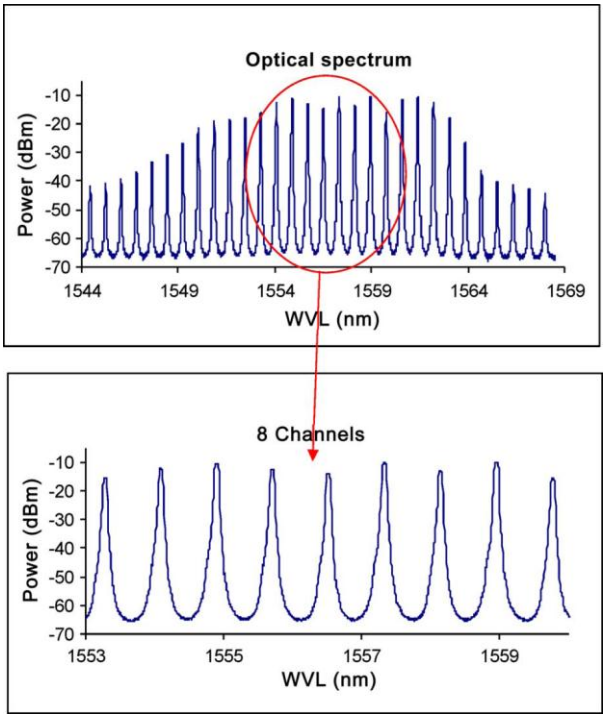

Figure 2.5: Optical spectrum of Fabry Perot (FP) mode locked lasers [9]

Yousra *et al.* [13] successfully demonstrated error free operation of 9 WDM channels with 100 GHz spacing using Q.Dash mode locker laser (MLL) with 56 Gb/s DQPSK modulation scheme. These mode locked (ML) lasers are also favorable for high speed optical networks for eliminating crosstalk due to the coherence of the MLL modes.

Short wavelength Q.Dot lasers is very suitable candidate for the all optical metropolitan access networks (MAN) where they extensively uses the wavelengths of O- band [14] and have some unique characteristics such as ultrafast gain recovery dynamics, pattern effect free amplification and efficient wavelength conversion based on four-wave mixing [15]. Meanwhile, for the further migration of WDM to short reach computer communication requires huge number of low cost economical laser and Q.Dot based mode locked laser (MLL) is one of the prominent candidates for such applications. Several advantages have been reported as high modal gain, ultra-broad emission spectrum and low noise characteristics, feasible high speed data transmission [16]. Hence, the mode locked lasers exhibit small pulse broadening in optical fibers but it has better threshold current density, temperature stability, and modulation characteristics compared to quantum well lasers [15, 17].

Kuntz *et al*. [15] demonstrated amplification of ultrafast 80 GHz 1.3μm Q.Dot optical combs and bit error rate (BER) free data signal amplification with 40 Gb/s Q.Dot semiconductor optical amplifiers (SOA) which is suitable for next generation Ethernet networks. Also, error free operation of some modes with a limited bandwidth of 3nm was first demonstrated for GaAs –based 1.3-μm quantum-dot (QD) laser [10, 18]. Most recently, a high performance tunnel injection quantum dot comb laser has been reported with a 75.9 nm FWHM bandwidth covering the short wavelength band [5]. The device

also shows superior temperature stability and small signal modulation bandwidth of 7.5 GHz. Though this Q. Dot MLL shows a great potential for several applications, further device and system level characterization would be essential for inventory purposes.

REFERENCES

[1] Semiconductor Laser Fundamentals Toshiaki Suhara, Osaka University, Japan, CRC Press 2004.

[2] Franois Lelarge; Batrice Dagens; Jeremie Renaudier; R. Brenot; Alain Accard; Frdric van Dijk; Dalila Make; Odile Le Gouezigou; Jean-Guy Provost; Francis Poingt; Jean Landreau; Olivier Drisse; Estelle Derouin; Benjamin Rousseau; Frdric Pommereau; Guang-Hua Duan; , "Recent Advances on InAs/InP Quantum Dash Based Semiconductor Lasers and Optical Amplifiers Operating at 1.55 μm," Selected Topics in -Quantum Electronics, IEEE Journal of , vol.13, no.1, pp.111-124, Jan.-feb. 2007.

[3] H. S. Djie and B. S. Ooi, X.-M. Fang, Y. Wu, J. M. Fastenau, W. K. Liu., and M. Hopkinson, "Room temperature broadband emission of InGaAs/GaAs quantum-dots laser," Opt. Lett., vol. 32, no. 1, January 1, 2007.

[4] H. S. Djie, C. L. Tan, B. S. Ooi, J. C. M. Hwang, X.-M. Fang, Y. Wu, J. M. Fastenau, W. K. Liu, G. T. Dang, and W. H. Chang, " Ultrabroad stimulated emission from quantum-dash laser", Appl. Phys. Lett. 91, 2007.

[5] Chi-Sen Lee, Wei Guo, Debashish Basu, and Pallab Bhattacharya, "High performance tunnel injection quantum dot comb laser "Appl. Phys. Lett. 96, 101107, 2010.

[6] C. Chen, G. Ding, B. Ooi, L. Lester, A. Helmy, T. Koch, and J. Hwang, "Optical injection modulation of quantum-dash semiconductor lasers by intra-cavity stimulated Raman scattering," Opt. Express 18, 6211-6219, 2010.

[7] Duan, Guang-Hua;, "InAs/InP based quantum dash mode-locked lasers for WDM transmission and millimeter wave generation," Communications and Photonics Conference and Exhibition (ACP), 2009 Asia , vol., no., pp.1-2, 2-6 Nov. 2009.

[8] Tan, C.L.; Djie, H.S.; Ooi, B.S.;, "Novel multiwavelength emitter for WDM transmission utilizing broadband quantum-dash laser diode," Lasers and Electro-Optics, 2009 and 2009 Conference on Quantum electronics and Laser Science Conference. CLEO/QELS 2009,pp.1-2, 2-4 June 2009.

[9] N. Yamamoto, et al., "Quantum Dot Optical Frequency Comb Laser with Mode-Selection Technique for 1-μm Waveband Photonic Transport System", Japanese Journal of Applied Physics, Volume 49, Issue 4, 2010.

[10] Akrout, A.; Shen, A.; Brenot, R.; Van Dijk, F.; Legouezigou, O.; Pommereau, F.; Lelarge, F.; Ramdane, A.; Guang-Hua Duan; , "Separate Error-Free Transmission of Eight Channels at 10 Gb/s Using Comb Generation in a Quantum-Dash-Based Mode-Locked Laser," Photonics Technology Letters, IEEE , vol.21, no.23, pp.1746-1748, Dec.1, 2009.

[11] Q. T. Nguyen, L. Bramerie, P. Besnard, A. Shen, A. Garreau, C. Kazmierski, G. H. Duan, and J. C. Simon, "24 channels colorless WDM-PON with L-band 10Gb/s downstream and C-band 2.5Gb/s upstream using multiple wavelengths seeding sources based on mode-locked lasers," in Conference on Optical Fiber Communications, Technical Digest (CD) (Optical Society of America, 2010), paper OThG6.

[12] R. Maher, K. Shi, L. Barry, J. o'Carroll, B. Kelly, R. Phelan, J. O?Gorman, and P. Anandarajah, "Implementation of a cost-effective optical comb source in a WDM-PON with 10.7Gb/s data to each ONU and 50km reach," Opt. Express 18, 15672-15681 (2010).
[13] Ben M'Sallem, Y.; Le, Q.T.; Bramerie, L.; Nguyen, Q.; Borgne, E.; Besnard, P.; Shen, A.; Lelarge, F.; LaRochelle, S.; Rusch, L.A.; Simon, J.; , "Quantum-Dash Mode-Locked Laser as a Source for 56-Gb/s DQPSK Modulation in WDM Multicast Applications," Photonics Technology Letters, IEEE , vol.23, no.7, pp.453-455, April1, 2011.
[14] D. Bimberg, M. Kuntz, and M. Laemmlin, BQuantum dot photonic devices for lightwave communication,[Appl. Phys. A,vol. 80, no. 6, pp. 1179–1182, 2005.
[15] Kuntz, M.; Fiol, G.; Laemmlin, M.; Meuer, C.; Bimberg, D.; , "High-Speed Mode-Locked Quantum-Dot Lasers and Optical Amplifiers," Proceedings of the IEEE , vol.95, no.9, pp.1767-1778, Sept. 2007.
[16] A. Kovsh et al, "Quantum dot comb-laser as efficient light source for silicon photonics", Proc. SPIE 6996, 2008.
[17] S. Fathpour, Z. Mi, and P. Bhattacharya, "High-speed quantum-dot lasers," J. Phys. D: Appl. Phys., vol. 38, pp. 2103–2111, 2005.
[18] T. Healy, F. C. G. Gunning, E. Pincemin, B. Cuenot, and A. D. Ellis,"1,200 km SMF, 100 km spans 280 Gbit/s coherent WDM transmission using hybrid raman/EDFA amplification," in Proc. Eur. Conf. Optical Communications, Berlin, Germany, Sep. 2007.

CHAPTER 3

EXPERIMENTAL DETAILS, SCOPE AND SETUP

The market demands are pushing the semiconductor industry to produce smaller, integrated and cost effective opto-electronic devices. To address these demands we have to design efficient optical sources which can be well implemented in the optical networks and short reach computer communications. Different researchers have opted for both short and long wavelength lasers as discussed in the previous section. One of these novel lasers [1] have been used as the focus for our study. In this chapter, we will discuss more about the experimental details, scope and setup used for the characterization of our novel emitter.

3.1 Details of the reported paper [1]:

Here multiwavelength high performance tunnel injection quantum dot laser has been characterized with 75.9nm FWHM bandwidth shown in the figure 3.1 (a). As the comb laser's channel spacing which is reported to be 0.1nm and 0.2 nm are dependent on cavity engineering, even with the change of temperature, channel spacing remains invariant as shown in figure 3.1 (b). One of the channels achieved modulation bandwidth of 7.5GHz.

The differential efficiency for the shorter cavity is found to be 52% and 40 % for the pulse and CW operation which proves that joule heating has a significant impact on efficiency degradation.

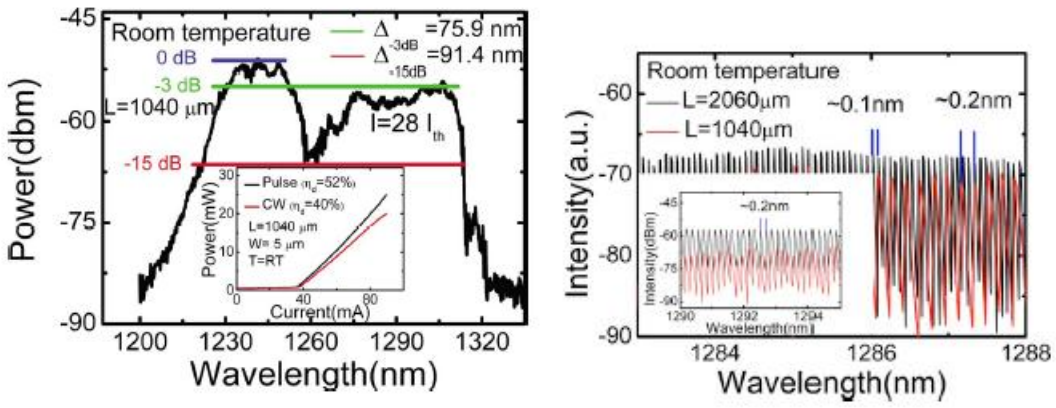

(a) (b)

Figure 3.1: EL spectra and channel spacing diagram [1]

Moreover, the T_0 and T_1 are found to be 110 and 300K. In the laser, the hot carrier effect and carrier leakage from the active layer have been significantly reduced with the aid of tunnel injection but it suffers from few drawbacks like electron–hole scattering and auger recombination due to the p-doping of the active layer. The threshold current density for the short cavity laser is reported to be 650 and 675 A / cm^2. There are few challenges as mentioned in the paper as:

1. Uniform and broadband gain from the active layer with a sufficiently large value of gain in the desired wavelength of interest.

2. Temperature stability of the output.

Therefore, we would like to address these issues in our experiment to understand the dynamics of this novel laser.

3.2 Scope of our experiments:

We will be looking into following facts for our experiment:

- ✓ Device performance with Pulse and CW injection and mode stability
- ✓ Effect of thermal conductivity in the device performance (internal quantum efficiency and external quantum efficiency) with different injections and temperature variations (internal quantum efficiency and external quantum efficiency)
- ✓ Characteristic temperature (T_0) and (T_1)
- ✓ -3dB and -15dB bandwidth performance under different injections
- ✓ Effects in shorter Cavity and longer Cavity

3.3 Sample preparation and setups:

We have used the following sample having surface contacts shown in figure 3.2 (a) and our experiment is carried over both short and long cavity (broad area) shown in figure 3.2 (b). Also, setup for the laser probing has been shown in figure 3.3 and schematic of overall setup is shown in figure 3.4.

One facet of our laser has been used to collect data through multimode fiber and another facet is used to collect the photons through an integrating Germanium photo-detector (PD) to study the L-I characteristics. There will be light emitted from both facets of the laser. The light emitted from one facet is coupled into a multimode fiber connected to optical spectrum analyzer to analyze the spectrum. The light emitted from the other facet is collected by an integrating sphere and measured by a Germanium photo-detector (PD). Temperature of laser station has been varied through the ILX laser diode controller.

Furthermore, the injections have been controlled through Labview – Keithley interface system through the software provided by the Keithley using a PC.

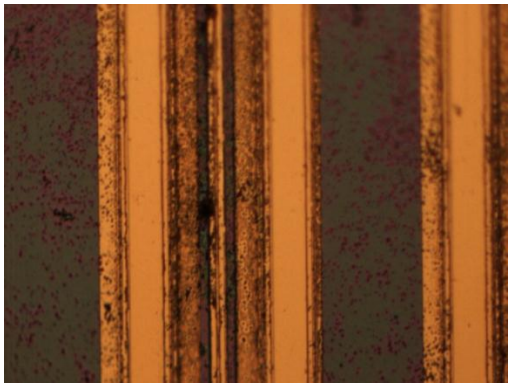

(a)

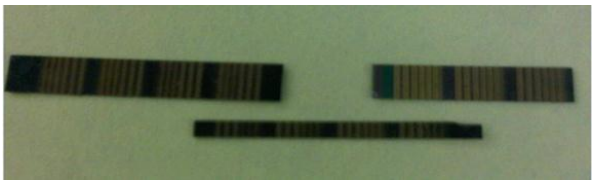

(b)

Figure 3.2: a) Ground-Signal-Ground (GSG) surface contacts, b) Shorter cavity and longer cavity

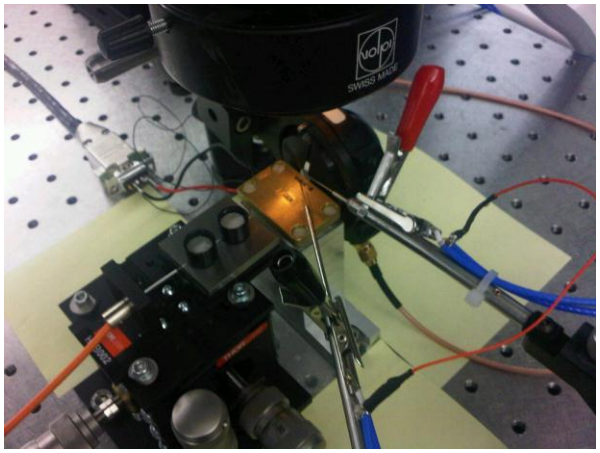

Figure 3.3: Setup of the probed laser

We have used setup values for 2 different kinds of cavities as follows and all our samples are tested as broad area laser. The setup values are summarized in table 3.1 and 3.2.

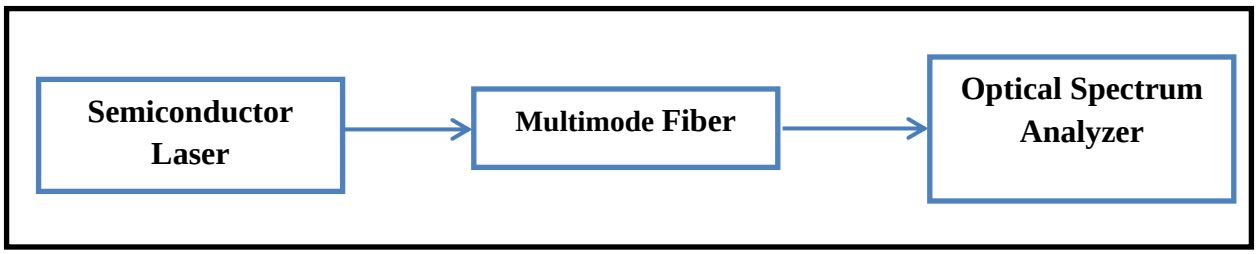

Figure 3.4: Diagram for the experimental setup.

Table 3.1: Basic setup values for longer cavity

Parameters	Values
Injection Current (Threshold)	90 mA for Pulse and 70 mA for CW Roll of happens: around 700mA
Width and Length	5 um and (~2mm)
Current Density (for 2mm)	873A/cm^2 and 679 A/cm^2
Temperatures	20-40 Degree C
Duty Cycles	1% to 30%
Current injection	1.5 to 6I_{th}
Bandwidth Observation	-3dB and -15 dB
Power (per facet) for 500mA pulse injection	153mW – 165mW for pulse operation

Table 3.2: Basic setup values for Shorter Cavity

Parameters	Values
Injection Current (Threshold)	40 mA for Pulse and 30 mA for CW Roll of happens: around 350mA
Width and Length	5 um and (~1mm)
Current Density (for 2mm)	769 A/cm^2 and 576 A/cm^2
Temperatures	20-40^{o}C
Duty Cycles	1% to 30%
Current injection	1.5 to 6I_{th}
Bandwidth Observation	-3dB and -15 dB
Power (per facet) for 500mA pulse injection	90mW- 150mW for pulse operation

3.4 Equations used for the experimental analysis

1. Threshold current density: It is an important parameter for the laser device and smaller threshold current density is preferred. Threshold current is not only dependent on the material but also on the width and size of the laser. Thus threshold current density (J = I / A) will be more appropriate rather than the threshold current.

2. Slope efficiency: it can be defined as equation (3.1),

$$\eta_i = \frac{dP}{dI} \qquad (3.1)$$

It tells us about the conversion rate between the electrical power inputs to the light power output. The higher the slope efficiency is better to characterize our device.

3. External quantum efficiency: It's a ratio between how many photons extracted out of the cavity with the injection and contributed to stimulated emission. As an example for the in-plane laser it can be 36 % and for VCSEL as 49% [2].

$$\eta_d = \left[\frac{q}{hv}\right]\frac{dP}{dI} \qquad (3.2)$$

4. Output power: The output power of the laser can be defined as in equation 3.3. Hence increasing the injection will cause the higher output till we reach to gain saturation. Meanwhile, the efficiency is dependent on the internal and external quantum efficiency.

$$P_{out} \propto \eta \frac{hv}{q}(I - I_{th}) \qquad (3.3)$$

5. Threshold gain: Threshold gain is a combination of internal loss and mirror loss. Following equations can be written to describe the threshold gain,

$$g_{th} = \alpha_i + \alpha_m \qquad (3.4)$$

$$\alpha_m = \frac{1}{L}\ln\frac{1}{R} \qquad (3.5)$$

$$\frac{\eta_i}{\eta_d} = 1 + \frac{\alpha_i}{\alpha_m} \qquad (3.6)$$

Internal loss is due to the loss of optical wave as the light propagates in the waveguide and mirror loss occurs at the facet. Nonradiative recombination of the carrier in the active layer causes internal loss.

6. Temperature dependency of laser is shown in equation 3.7. As the temperature increase threshold current increases exponentially.

$$I \propto e^{(T / To)} \qquad (3.7)$$

In the following chapters, we will discuss more about our experimental findings.

REFERENCES

[1] Chi-Sen Lee, Wei Guo, Debashish Basu, and Pallab Bhattacharya, "High performance tunnel injection quantum dot comb laser "Appl. Phys. Lett. 96, 101107, 2010.
[2] L. A. Coldren and S. W. Corzine, Diode Lasers and Photonic Integrated Circuits, New York: Wiley, 1995
[3] Mobrahan, Kamran S: Test and Characterization of Laser Diodes: Determination of Principal Parameters", Application Note, Newport, CVR2, 1999.

CHAPTER 4
EXPERIMENTAL FINDINGS

4.1 Duty Cycle Based Characterization of Multiwavelength High Performance Quantum Dot Comb Laser

As reported, Quantum well and Quantum Dot devices wavelengths increase with the duty cycle and temperature due to the lattice heating as shown in figure 4.1.1 [1]. Figure 1 clearly shows the dependence of wavelength shift due to the change in duty cycle which proves the effect of thermal conductivity in the active layer. Also InGaAs – GaAs based Quantum Dot laser shows unusual sensitivity of chirp to the duty cycle of the current which is the effect of low thermal conductivity of Q.Dot regions and increased thermal effects of those devices as shown in figure 4.1.2 [2].

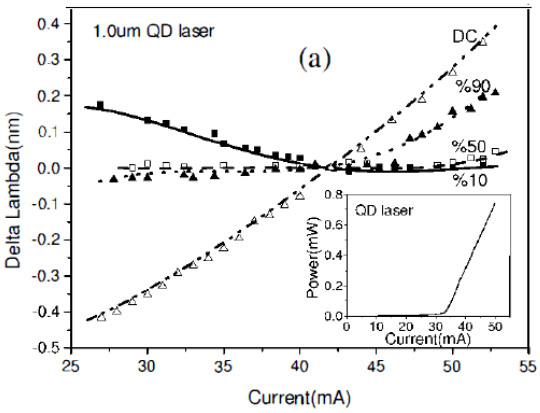

Figure 4.1.1: Change of wavelength with the increment of duty cycle [1]

Depending on the application, this novel laser needs to act on CW / Quasi-CW / pulse time regimes. The majority of the literature reports that the operation pulse is below ~ 1% but the other time regimes are yet to be reported. Consequently in this chapter, further

experiments have been carried out based on different duty cycles such as pulse, quasi-cw and cw based injection to demonstrate the thermal conductivity of this high performance comb laser spectrum in the different operational regime which has not been reported yet.

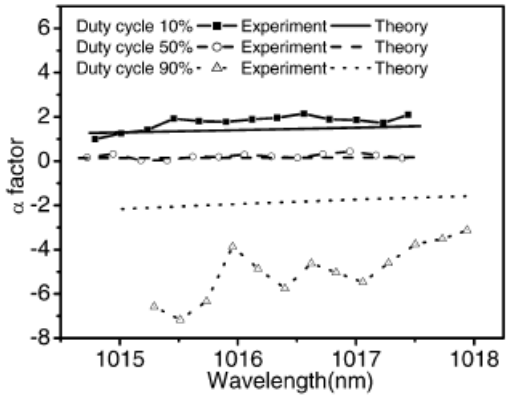

Figure 4.1.2: Consequence of higher duty cycle [2]

Experimental analysis for long cavity Quantum Dot Laser:

In the first part, we did the characterization by varying the duty cycle with constant temperature and for the second part we tried to observe the effect by varying the temperature in pulse and CW regime from the single facet of the cavity. All the performances will be evaluated through slope efficiency, differential quantum efficiency and threshold current density for both of the 1mm as well as 2mm long cavity.

a. Threshold current density

In the table 4.1 and 4.2, we have summarized the threshold current density for both of the cavities with pulse / cw injection.

Table 4.1: For 2mm long cavity Laser

Type of injection	Threshold current	Current Density
Pulse	90mA	873 A/cm^2
CW	70mA	679 A/cm^2

Table 4.2: For 1mm long cavity Laser

Type of injection	Threshold current	Current Density
Pulse	40mA	769 A/cm^2
CW	30mA	576 A/cm^2

The threshold current at room temperature for long cavity is found to be higher than the shorter one but the difference in threshold current density is not much varied. We can see from the following equations that, threshold current is also dependent on the length. As our cavity length does not differ greatly, the total current density change is also negligible. Usually the threshold current decreases with the cavity length and it increases drastically until it reaches below the optimum length as reported in one of the literatures [**3**].

$$I_{th} = (J_{th} \sim \text{modal gain}) \times L \times \text{width} \quad (4.1)$$

Internal losses due to the auger recombination and p-doping in the active layer might have significant contributions for the increased threshold current density for these set of lasers.

b. L-I characteristics and efficiency

Figures 4.1.3 and 4.1.4 represent the L-I characteristics of short cavity at low duty cycle for the range from 1 to 5% whereby the linear relationship above the threshold current remains constant apart from the small deviation in the 1 mm short cavity. Simultaneously figures 4.1.5 and 4.1.6 can be regarded as the L-I characteristics for both cavities respectively in the quasi – cw regime whereby we can see a clear detrition for the short cavity (1mm) laser due to the heating effect of the higher duty cycle injection. The roll off current observed for 1mm short cavity broad area laser is at 350 mA for higher duty cycle operation. From the slope of these L-I characteristics we will be able to do further analysis on the internal and differential (external) quantum efficiency of these laser diodes.

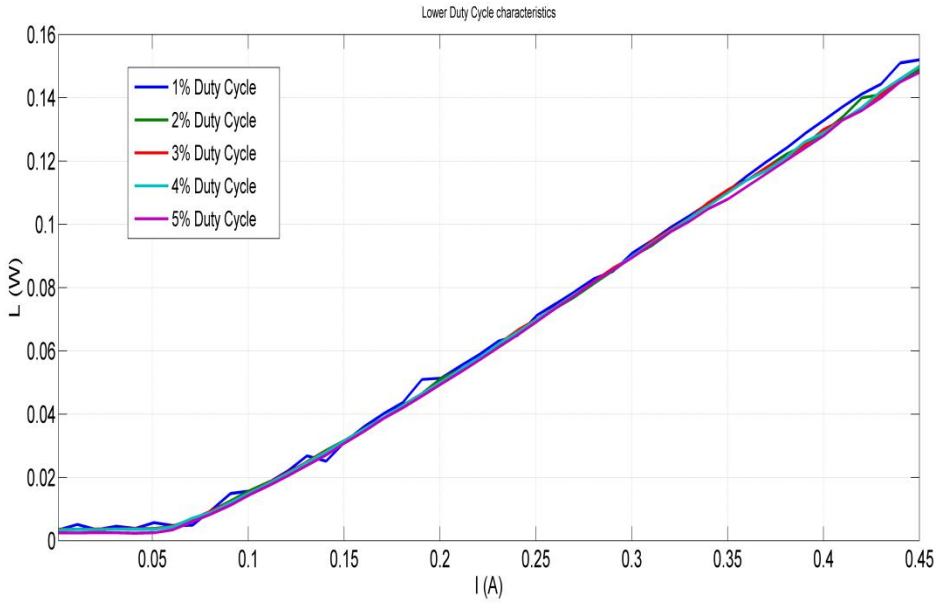

Figure 4.1.3: L-I Characteristics for the lower duty cycle operations (2mm Cavity)

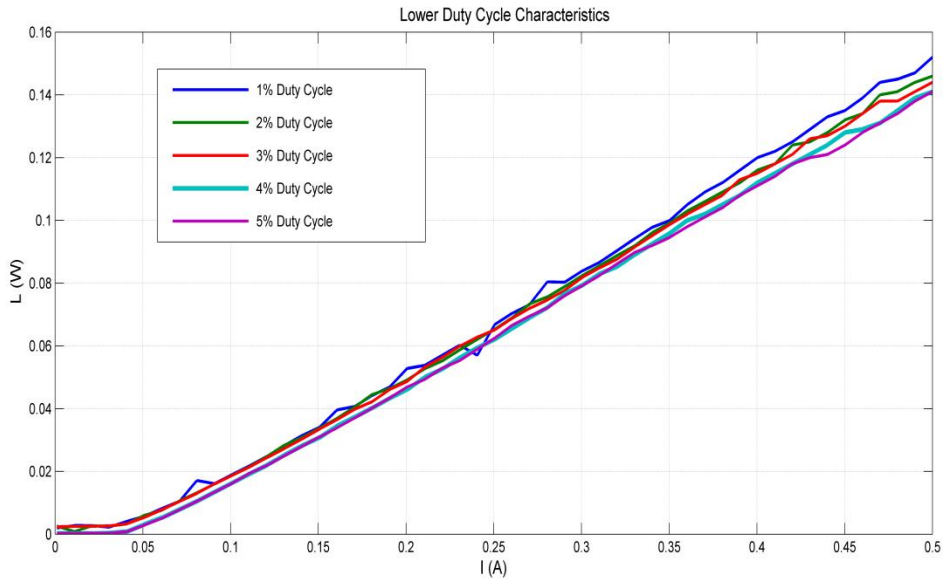

Figure 4.1.4: L-I Characteristics for the lower duty cycle operations (1mm Cavity)

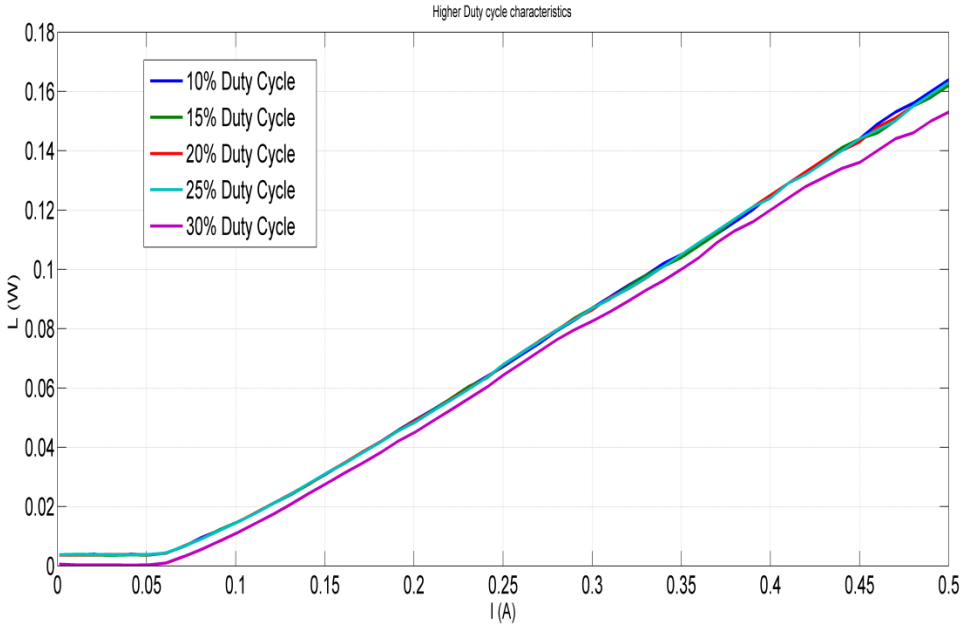

Figure 4.1.5: L-I Characteristics for the higher duty cycle operations (2mm Cavity)

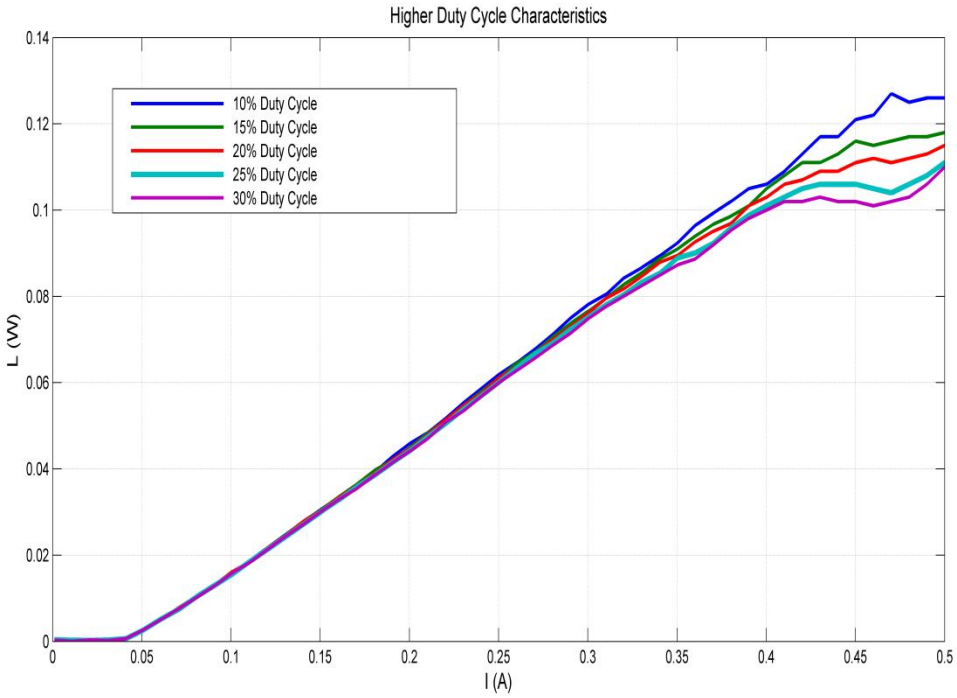

Figure 4.1.6: L-I Characteristics for the higher duty cycle operations (1mm Cavity)

Depending on the situations, we observed decrease in slope efficiency indicating that the device performance degradation is temperature dependent [4]. For the lower duty cycle operation, we have observed similar phenomena as well as the differential quantum efficiency decrease shown in table 4.3. With the higher duty cycle injection, the performance degrades further as depicted in table 4.4. The typical threshold current is recorded as 90mA for the pulse and 70mA for the CW operation at the room temperature operation (19^{o}C) for the longer cavity. Table 4.5 and 4.6 shows the results for the 1 mm cavity where we have seen severe degradation of efficiency. For the smaller cavity it reaches to 34% from 39% and with higher duty cycle / quasi pulse operation 37% to 31%. Even at the highest duty cycle the drop is around 10% compared to the longer one.

The reasons behind these phenomena will be described in the analysis and discussion chapter. Hence, all the results shown in the table depict efficiency for per facet and is needed to be multiplied by 2 to know the total efficiency for each of the conditions.

Table 4.3: Study based on the lower duty cycle 2mm Cavity: (Temp: 19^{o}C)

Duty cycle	**Slope efficiency per facet**	**Differential quantum efficiency per facet**
1%	39.05%	39.74%
2%	38.91%	39.64%
3%	38.96%	39.52%
4%	38.96%	39.69%
5%	38.31%	39%

Table 4.4: Study based on the higher duty cycle 2mm Cavity: (Temp: 19^{o}C)

Duty cycle	**Slope efficiency per facet**	**Differential quantum efficiency per facet**
10%	37.81%	38.81%
15%	37.40%	38.07%
20%	37.81%	38.44%
25%	37.45%	38.09%
30%	37.22%	38.18%

Following table 4.5 and 4.6 show the results for the shorter cavity (1mm) in lower and higher duty cycle regime. Threshold current is around 40mA for the shorter cavity.

Table 4.5: Study based on the lower duty cycle for 1mm cavity: (Temp: 19^{o}C)

Duty cycle	**Slope efficiency per facet**	**Differential quantum efficiency per facet**
1%	33.82%	34.69%
2%	33%	34.03%
3%	32.62%	33.73%
4%	33.01%	34.02%
5%	32%	32.97%

Table 4.6: Study based on the higher duty cycle for 1mm cavity: (Temp: 19^{o}C)

Duty cycle	**Slope efficiency per facet**	**Differential quantum efficiency per facet**
10%	31.39%	32.40%
15%	30.25%	31.22%
20%	29.72%	30.58%
25%	28.62%	29.56%
30%	27.91%	28.83%

Section Summary:

In general, we have tried to observe the thermal conductivity of the active region of this short wavelength laser based on duty cycle imposed pulse / continuous injection for 2mm

and 1mm cavity length. These results will be used to analyze the performance of the laser. Important findings are summarized as below:

1. Threshold current density is almost the same for the both of the cavities.

2. Performance degradation is severe for smaller cavity compared to the longer cavity as reported that the auger recombination in the shorter cavity is the dominant one and for the longer cavity, radiative and interface recombinations are the dominant one [3].

3. In both of the cases, slope efficiency decreases with the increment of duty cycle which proves the thermal conductivity effect in the active layer [4].

REFERENCES

[1] Tan, H.; Kamath, K.; Bhattacharya, R.; Klotzkin, D., "Evidence for reduced thermal conductivity in quantum dot active region from chirp characteristics in InGaAs/GaAs quantum dot lasers," Lasers and Electro-Optics Society, LEOS 2004. The 17th Annual Meeting of the IEEE , vol.2, no., pp. 619- 620 Vol.2, 7-11 Nov. 2004.

[2] Hua Tan; Zetian Mi; Bhattacharya, P.; Klotzkin, D.; , "Dependence of Linewidth Enhancement Factor on Duty Cycle in InGaAs–GaAs Quantum-Dot Lasers," Photonics Technology Letters, IEEE , vol.20, no.8, pp.593-595, April15, 2008.

[3] Johnson Lee, C. Shieh, and M. O. Vassell, “Variation of threshold current with cavity length in strained-layer InGaAs/GaAs quantum well lasers,” J. Appl. Phys. 69, 1882, 1991.

[4] Tan, H.; Kamath, K.; Bhattacharya, R.; Klotzkin, D.; , "Evidence for reduced thermal conductivity in quantum dot active region from chirp characteristics in InGaAs/GaAs quantum dot lasers," Lasers and Electro-Optics Society, LEOS 2004. The 17th Annual Meeting of the IEEE , vol.2, no., pp. 619- 620 Vol.2, 7-11 Nov. 2004.

4.2 Temperature Variance Characterization of Multiwavelength High Performance Quantum Dot Comb Laser

Due to the extensive growth and convergence of high speed data networks, short wavelength Quantum Dot (Q.Dot) lasers will be a vital player in the transmitter industry. Though dynamic and static heating is a prominent problem for the quantum well lasers [1] quantum dot (Q.Dot) lasers are expected to show superior performance such as higher temperature stability, higher modulation bandwidth, and lower threshold currents due to the presence of discrete energy states. Performance of Q.Dot lasers degrades due to the presence of excited states and inhomogeneous broadening as the Q.Dot size fluctuates [**2**]. Hence, integration of such low dimensional Q.Dot lasers requires stable threshold current density and differential quantum efficiency for future applications. Therefore, in this chapter we have briefly observed the performance of temperature variance characterization of multiwavelength high performance Quantum Dot Comb Laser. Also the characteristic temperature is being shown for both of the cavities in the later section.

Here, the experiment is done for 1mm and 2mm laser cavity for 1% and 20 % duty cycle rate. For both of the cavities, we have varied the temperature to study the temperature dependency of such novel lasers. The temperature variation is made from 20^{o}C to 40^{o}C using ILX temperature controller module. Tables 4.7 and 4.8 summarize the quantum efficiency and figures 4.2.1-4.2.4 shows the L-I characteristics for the both cavities.

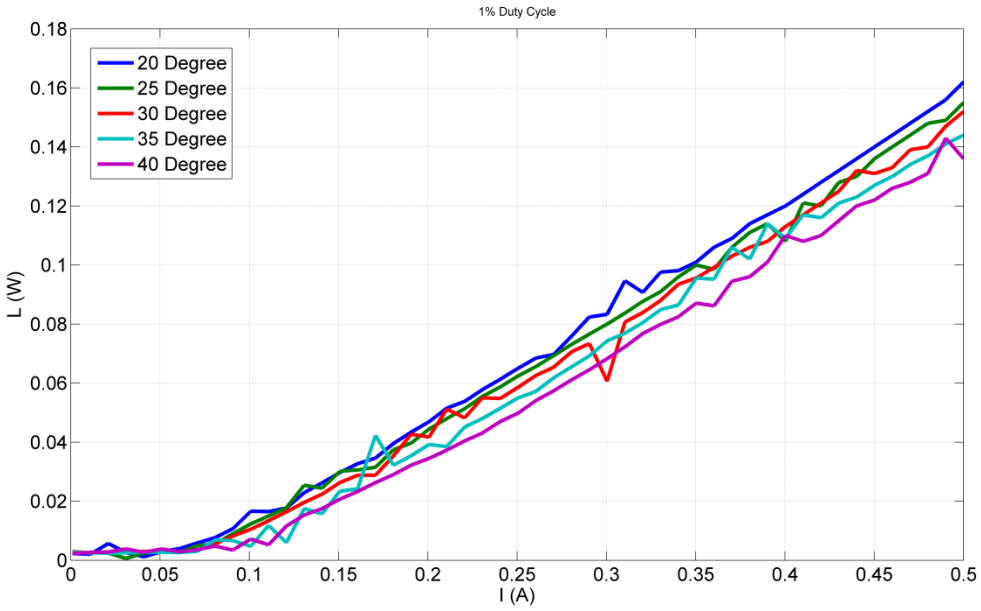

Figure 4.2.1: L-I Characteristics of temperature variation with the lower duty cycle injection (2mm Cavity)

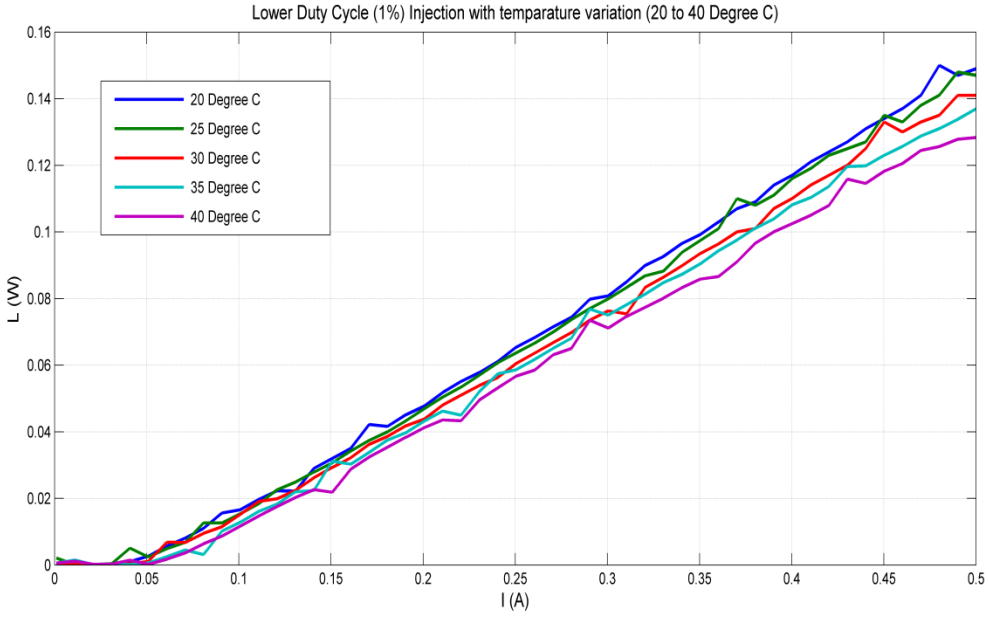

Figure 4.2.2: L-I Characteristics of temperature variation with the lower duty cycle injection (1mm Cavity)

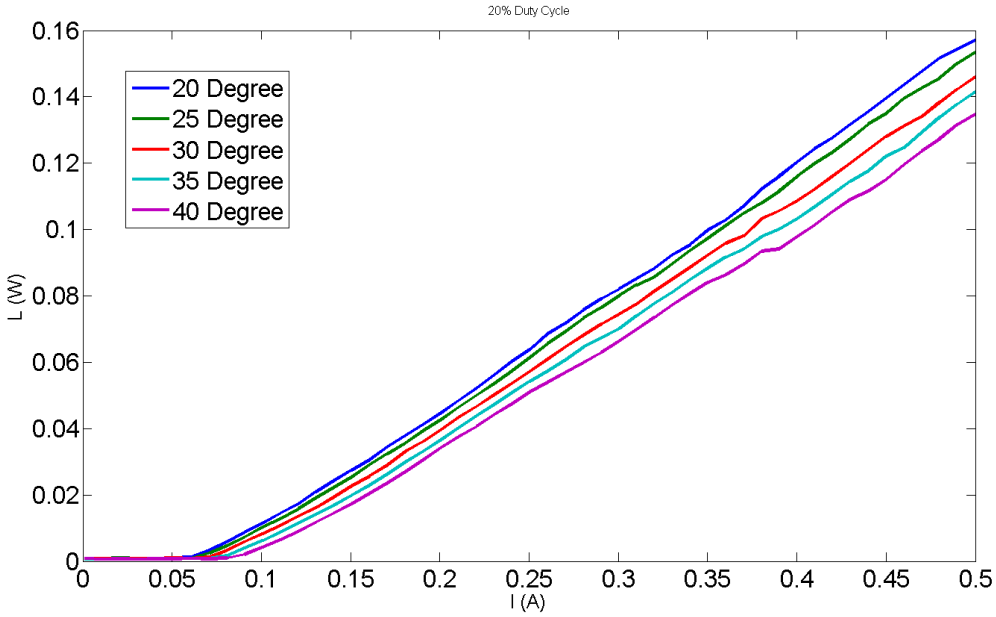

Figure 4.2.3: L-I Characteristics of temperature variation with the higher duty cycle injection (2mm Cavity)

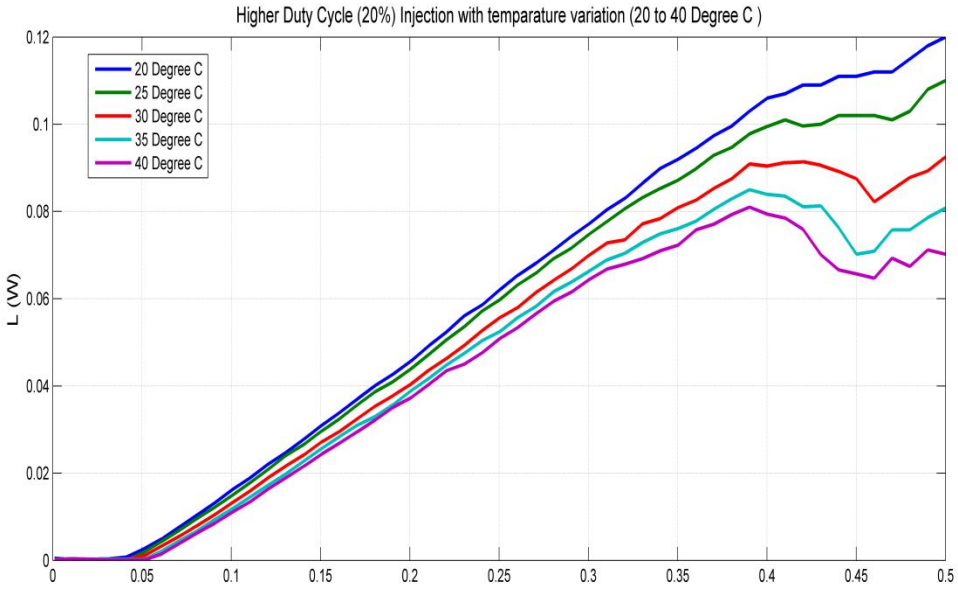

Figure 4.2.4: L-I Characteristics of temperature variation with the higher duty cycle injection (1mm Cavity)

From L-I characteristics we have observed that (figures 4.2.1 to 4.2.4), the performance remains quite stable for the lower duty cycle for both cavities with temperature variations but at the elevated temperature with the presence of higher duty cycle, the smaller cavity is affected adversely. Hence the findings will be more prominent with the results in quantum efficiency which has been depicted in tables 4.7 and 4.8.

Table 4.7: Temperature Dependent Study of 2mm longer cavity:

	Duty Cycle 1%		**Duty Cycle 20%**	
Temperature	**Slope Efficiency per facet**	**Differential Quantum Efficiency**	**Slope Efficiency per facet**	**Differential Quantum Efficiency**
20^{o}C	37.01%	38.20%	37.43%	38.29%
25^{o}C	34.13 %	35.28%	36.62%	37.53%
30^{o}C	36.68%	37.96%	34.71%	35.88%
35^{o}C	36%	37.36%	33.23%	34.44%
40^{o}C	35.17%	36.59%	32.22%	33.47%

Table 4.8: Temperature Dependent Study of 1mm shorter cavity:

	Duty Cycle 1%		**Duty Cycle 20%**	
Temperature	**Slope Efficiency per facet**	**Differential Quantum Efficiency**	**Slope Efficiency per facet**	**Differential Quantum Efficiency**
20^{o}C	33.87%	34.55%	30.29%	30.73%
25^{o}C	33.54%	34.27%	28.67%	29.24%
30^{o}C	32.01%	32.88%	26.43%	27.20%
35^{o}C	30.10%	31.04%	24.85%	25.73%
40^{o}C	30.90%	32.09%	24.52%	23.29%

Table 4.7 and table 4.8 depict the temperature dependent performance for both of the 2 mm and 1 mm cavity. The performance degradation observed for the longer cavity is in the range of 2 to 4% but for the shorter cavity the range has been prolonged to 3 to 10% which proves that smaller cavity is less resilient to the higher temperature which might be due to the resistive heating of injection as well as for the radiative recombination. This situation also contributes to the higher threshold current for the laser operation. Further details will be incorporated in the discussion chapter.

Characteristic temperature of the Comb Laser

Determining the characteristic temperature for the laser is very important because the increment of temperature affects the performance of the operating laser. The characteristic temperature (T_0) can be derived from L-I curve. We will see that increasing the temperature also increases the threshold current. T_o adjusts with the formulation as equation 4.2 as we have to consider two temperatures where one should be 20 and the other one is 85^o C [3]. For our experiment, the highest temperature is set as 40^{o}C due to the device limitations in the temperature controller.

$$T_0 = \frac{T\,high - Tlow}{In\left(\frac{I_{high}}{I_{low}}\right)} \tag{4.2}$$

Here the highest and lowest temperature is 20 and 40^{o}C respectively and the lower as well as upper bound for the threshold current is 50mA and 120mA. Based on the equation 4.2 the calculated T_0 is 295K and T_1 is around 303K for the longer cavity. For better stability higher T_1 is always desired. The reported characteristic temperature is higher

than the typical value of 50K due to P-doping of the dots which increases electron-hole scattering and auger recombination rate [**4**].

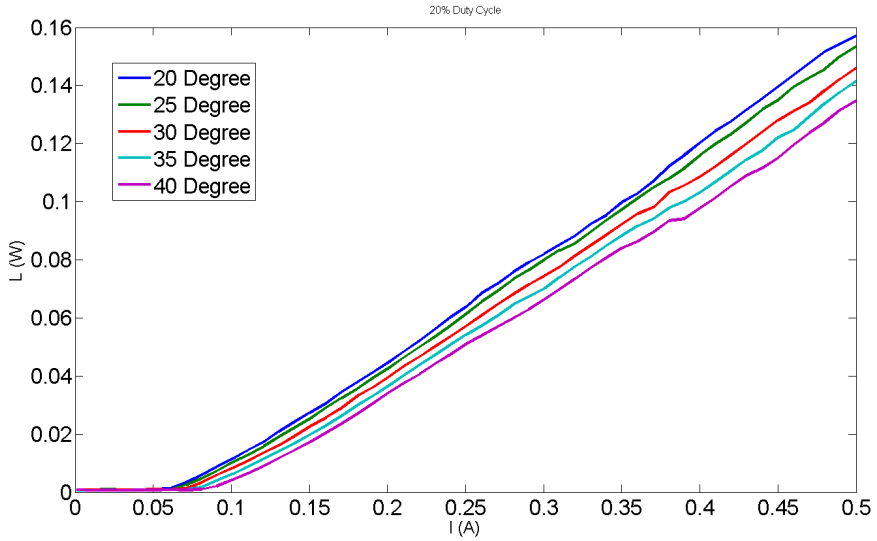

Figure 4.2.5: L-I characteristics for the higher duty cycle with elevated temperatures

Section Summary:

In general, we have tried to observe the thermal conductivity with the presence of elevated temperature for the 2mm and 1mm cavities which indicated the performance trends of the novel laser. Important findings are summarized as below:

1. With elevated temperature, shorter cavity's efficiency drops drastically compared to the longer one. As the temperature increases higher, the non-radiative recombination occurs more subsequently and efficiency drops.

2. The characteristic temperature is found to be higher than the conventional laser as reported [4] due to the P-doping in the active layer.

REFERENCES

[1] D. Klotzkin and P. Bhattacharya, "Temperature Dependence of Dynamic and DC Characteristics of Quantum-Well and Quantum-Dot Lasers: A Comparative Study," J. Lightwave Technol. 17, 1634-, 1999.

[2] Yulian Cao, Tao Yang, Haiming Ji, Wenquan Ma, Qing Cao, Lianghui Chen, "Temperature Sensitivity Dependence on Cavity Length in p-Type Doped and Undoped 1.3-μm InAs–GaAs Quantum-Dot Lasers", Photonics Technology Letters, IEEE, On page(s): 1860 - 1862, Volume: 20 Issue: 22, Nov.15, 2008.

[3] Ing. Radek KVÍČALA, "TEMPERATURE DEPENDENCY OF SEMICONDUCTOR LASER", Doctoral Degree program, visited on 24th Sept, 2011; online link: (http://www.feec.vutbr.cz/EEICT/2005/sbornik/03-Doktorske_projekty/01-Elektronika/14-xkvica00.pdf), 2011.

[4] Chi-Sen Lee, Wei Guo, Debashish Basu, and Pallab Bhattacharya, "High performance tunnel injection quantum dot comb laser "Appl. Phys. Lett. 96, 101107, 2010.

4.3 Spectrum Behaviors and Cavity Engineering of Quantum Dot Comb Lasers

LAtely, semiconductor broadband lasers have attained attention due to the possible implementation in sensor applications, medical imaging and low cost computer communication system. Such devices are compact and energy efficient which made them more prominent over the power hungry systems. One of such examples is a recently reported high speed multiwavelength Quantum Dot laser grown by molecular beam epitaxy (MBE), characterized with 75.9 nm (FWHM) and 91.4 nm (-15dB bandwidth) wide lasing spectrum [1]. Hence in this chapter we will observe the broadband emission from lasers with electrical injection for longer and shorter cavity. Also, the channel spacing stability for the longer cavity with different duty cycle based pumping will be investigated.

4.3.1 Spectrum Behaviors

We have designed our experiment for both shorter (1mm) and longer cavity (2mm) and also taken the pumping considerations shown in the table 4.9 and 4.13 for the shorter and longer cavity. For our experiment, we have analyzed full wave half maximum (FWHM = - 3dBm) and -15 dBm bandwidth. -15dBm bandwidth is observed here because the experiment suffers from lot of losses such as waveguide losses, coupling losses etc. This total loss can be accounted for by ideal bandwidth measurement. Therefore, observing -15dBm bandwidth is required.

Table 4.9: Different injection levels for longer cavity (2mm) - Threshold current (50-70mA)

1% Duty cycle pulse injection	15% Duty cycle pulse injection	CW based injection
150 mA	150 mA	150 mA
210 mA	210 mA	210 mA
280 mA	280 mA	280 mA
350 mA	350 mA	350 mA
400 mA	400 mA	400 mA

Table 4.10: Bandwidth for 1 % Duty cycle pumping

Injection current	Peak wavelength (nm)	Bandwidth (-3 dBm)	Bandwidth (-15dBm)
150 mA	1285.1881	~ 6nm	~ 14nm
210 mA	1287.9538	~10nm	~23nm
280 mA	1272.9493	~ 6nm	~34nm
350 mA	1274.5112	~ 7nm	~10nm
400 mA	1267.2921	~ 11nm	~28nm

Table 4.11: Bandwidth for 15 % Duty cycle pumping

Injection current	Peak wavelength (nm)	Bandwidth (-3 dBm)	Bandwidth (-15dBm)
150 mA	1281.0172	~16nm	~ 19nm
210 mA	1292.9824	~22nm	~ 28nm
280 mA	1262.8108	~15nm	~23nm
350 mA	1276.0198	~8nm	~30nm
400 mA	1271.8664	~9nm	~ 32nm

Table 4.12: Bandwidth for CW pumping

Injection current	Peak wavelength (nm)	Bandwidth (-3 dBm)	Bandwidth (-15dbm)
150 mA	1289.2610	~ 8nm	~10nm
210 mA	1304.1338	~ 4nm	~18nm
280 mA	1289.3900	~ 3nm	~ 6nm
350 mA	1303.2395	~ 2nm	~ 8nm
400 mA	1336.5734	~ 2nm	~ 9nm

Here tables 4.10-4.12 shows the bandwidths for the longer cavity at different pumping levels. As the threshold current level is between 50-70 mA, we restricted the pumping level to 400mA for the longer cavity laser. Table 4.10 shows a steady bandwidth for the low duty cycle injection but on the contrary the bandwidth decreases with higher duty cycle (15% and CW) possibly due to the contributions of non-radiative recombination and heating effects. For the 400 mA pumping with 1% duty cycle, the bandwidth tends to increase by 4 nm. Hence we have observed the least bandwidth for CW based injection which in around 2 nm for the 400 mA injection.

From the table 4.10-4.12, it is clear that the FWHM bandwidth (-3dBm) is decreasing with the increment of pumping current. But there is considerable amount of bandwidth (-15 dBm) for 15% duty cycle pumping and least significant bandwidth for the CW pumping. For the longer cavity, when the duty cycle approaches CW regime, not only the power drops but also the bandwidth drops consequently. A similar investigation has been done for the shorter cavity. The following table 4.13 shows the different injection levels for the shorter cavity. As we have observed the threshold current to be in the range of 30-50 mA we have restricted the total pumping level to 350 mA.

For the shorter cavity (table 4.14-4.16), a similar trend is observed as shown in the table 4.14 but there is a considerable amount of the -15 dBm bandwidth increase with the increasing injection level. But for the 15% pumping level, the FWHM trend is different than the longer cavity. In this scenario, the FWHM bandwidth increases with pumping level. But for the CW electrical pumping with higher injection rates (e.g. 350 mA), the lasing ceases as shown in figure 4.3.3. This signifies that, with the higher pumping we are

able to receive the broader bandwidth but the power drops due to the heat induced effects and non-radiative recombinations.

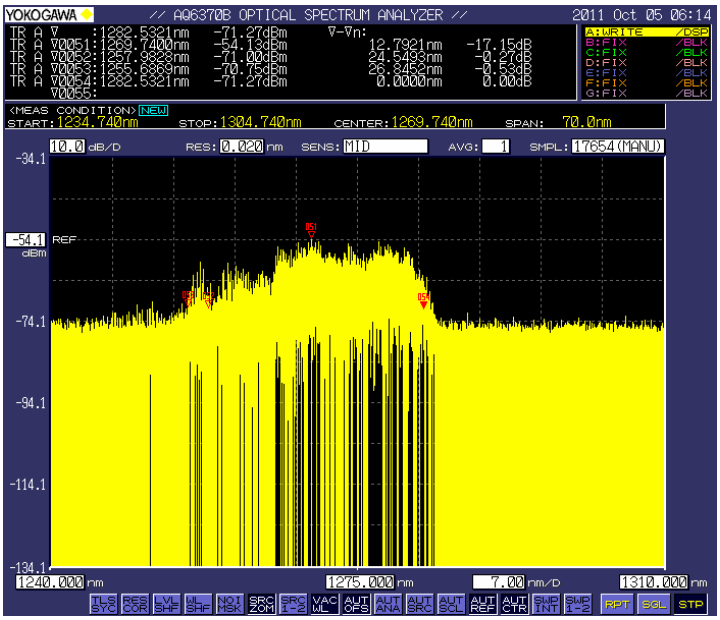

Figure 4.3.1: Spectrum for 1% duty cycle pumping with 400 mA

Table 4.13: Different injection levels for shorter cavity (1mm) - Threshold current (30-50mA)

1% Duty cycle pulse injection	15% Duty cycle pulse injection	CW based injection
120 mA	120 mA	120 mA
180 mA	180 mA	150 mA
250 mA	250 mA	180 mA
350 mA	350 mA	250 mA
-	-	350 mA

Table 4.14: Bandwidth for 1 % Duty cycle pumping

Injection current	**Peak wavelength (nm)**	**Bandwidth (-3 dBm)**	**Bandwidth (-15dBm)**
120 mA	1276.02	~ 15nm	~ 19nm
1**8**0 mA	1276.0040	~ 3nm	~ 23nm
250 mA	1276.0640	~ 3nm	~ 22nm
350 mA	1276.0320	~ 4nm	~ 31nm

Table 4.15: Bandwidth for 15 % Duty cycle pumping

Injection current	**Peak wavelength (nm)**	**Bandwidth (-3 dBm)**	**Bandwidth (-15dBm)**
120 mA	1276.1000	No significant spectrum range	~ 13nm
1**8**0 mA	1277.9560	No significant spectrum range	~ 18nm
250 mA	1272.7520	~ 11nm	~ 28nm
350 mA	1279.38	~ 18nm	~ 27nm

Table 4.16: Bandwidth for CW pumping

Injection current	**Peak wavelength (nm)**	**Bandwidth (-3 dBm)**	**Bandwidth (-15dbm)**
120 mA	1286.0560	~ 2nm	~ 9nm
150 mA	1293.4931	~ 7nm	~ 12nm
180 mA	1296.8760	~ 13nm	~ 15nm
250 mA	1320.0400	~ 3nm	~ 4nm
350 mA	-	-	-

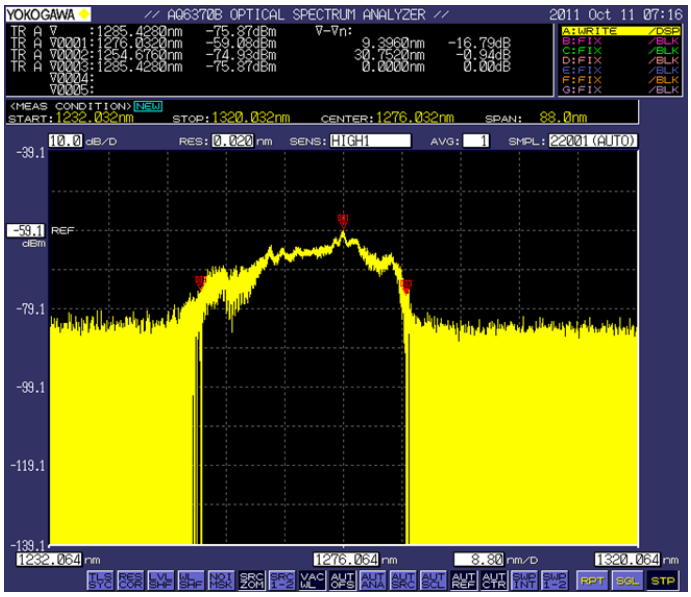

Figure 4.3.2: Spectrum for 1% duty cycle pumping with 350 mA

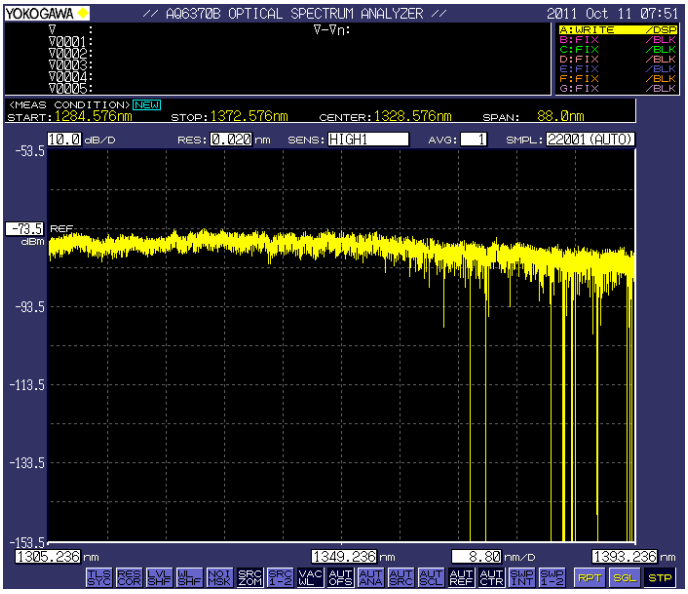

Figure 4.3.3: lasing ceases at 350mA injection for CW pumping.

Furthermore, with the aid of cavity engineering we can design the channel spacing which can be used for widely implemented WDM / DWDM networks. Typical Dense WDM (DWDM) systems use the channel spacing from 0.1 nm (12.5 GHz) to 0.8nm (100 GHz)

[2]. The following example as table 4.17 (a) - (b) show the bandwidth observed in the longer cavity which can be implemented in the optical networks as shown below.

Table 4.17: Possible implications in the system level

a) For 15% Duty cycle pulse injection (DWDM – 0.4 nm spacing and HDWDM - .1 nm spacing)

Bandwidth (-3 dBm)	**DWDM realization**	**HDWDM realization**	**Bandwidth (-15dbm)**	**DWDM realization**	**HDWDM realization**
~16nm	20 channels	160 channels	**~ 19nm**	25 channels	190 channels
~22nm	10 channels	220 channels	**~ 28nm**	45 channels	280 channels
~15nm	7 channels	150 channels	**~23nm**	15 channels	230 channels
~8nm	5 channels	80 channels	**~30nm**	20 channels	300 channels
~9nm	5 channels	90 channels	**~ 32nm**	22 channels	320 channels

b) For CW injection (DWDM – 0.4 nm spacing and HDWDM - .1 nm spacing)

Bandwidth (-3 dBm)	**DWDM realization**	**HDWDM realization**	**Bandwidth (-15dbm)**	**DWDM realization**	**HDWDM realization**
~ 8nm	20 channels	80 channels	**~10nm**	25 channels	100 channels
~ 4nm	10 channels	40 channels	**~18nm**	45 channels	180 channels
~ 3nm	7 channels	30 channels	**~ 6nm**	15 channels	60 channels
~ 2nm	5 channels	20 channels	**~ 8nm**	20 channels	80 channels
~ 2nm	5 channels	20 channels	**~ 9nm**	22 channels	90 channels

5.3.2 Cavity Engineering

The channel spacing can be engineered with the aid of cavity length size which maintains the reciprocal relationship known as cavity engineering. Hence, for our case we tried to observe the effect of cavity engineering for the longer cavity (~ 2mm).

Channel spacing for the broadband lasers can be engineered as $\lambda^2 / 2nL$ which relies on a reciprocal relationship. Therefore by taking peak wavelength = 1272.29 nm, n = 3.65, cavity length = 2048μm; the channel spacing range might be varied from .10nm to 0.12 nm. But due to the thermal activity in the active region; the channel spacing uniformity might not be well maintained as performance degradation occurs due to the thermal escape of carriers and temperature sensitive internal loss [3]. Here figure 4.3.4 shows the channel spacing uniformity for the longer cavity in all possible scenarios. From the figure, it's quite obvious that uniformity is attained when the pumping rate is higher. The uniform channel spacing is gained at CW pumping. Figures 4.3.5-4.3.7 show the channel spacing uniformity of the comb spectrums for the 30% pulse, CW 320 mA and 350 mA injections respectively. With the higher injection, the comb spectrum gains more stable uniformity than the one shown in figure 4.3.4.

Hence, we fixed the injection at 400 mA and varied the temperature to 20, 30, and 40^{o}C to see the impact on channel spacing uniformity with the temperature variation. From figure 4.3.8 we can see that the uniformity deviates when the temperature goes higher due to heating. In general, the broadband spectrum shows red shift with alleviation of temperature.

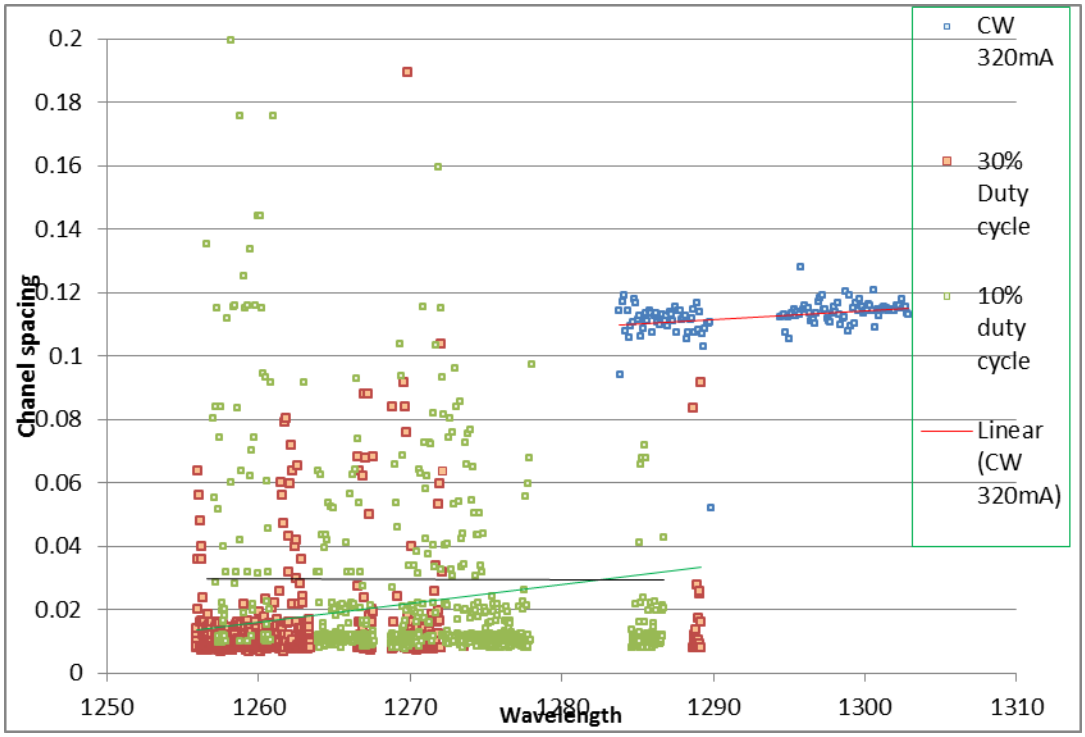

Figure 4.3.4: Channel spacing uniformity for the longer cavity

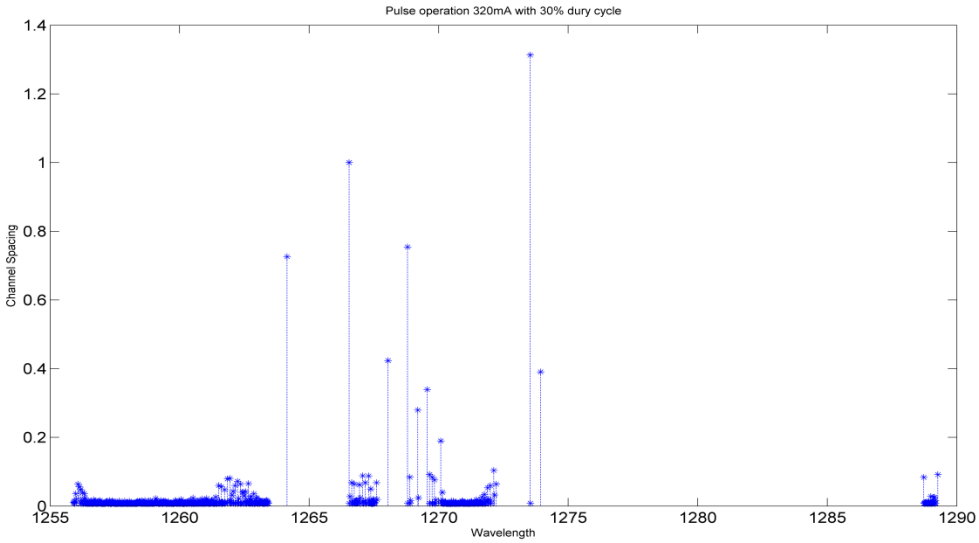

Figure 4.3.5: Pulse injection

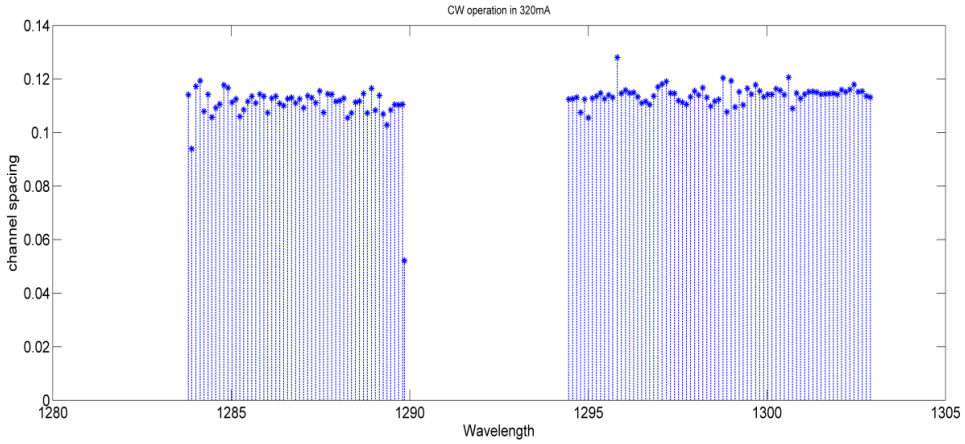

Figure 4.3.6: CW operation with 320 mA

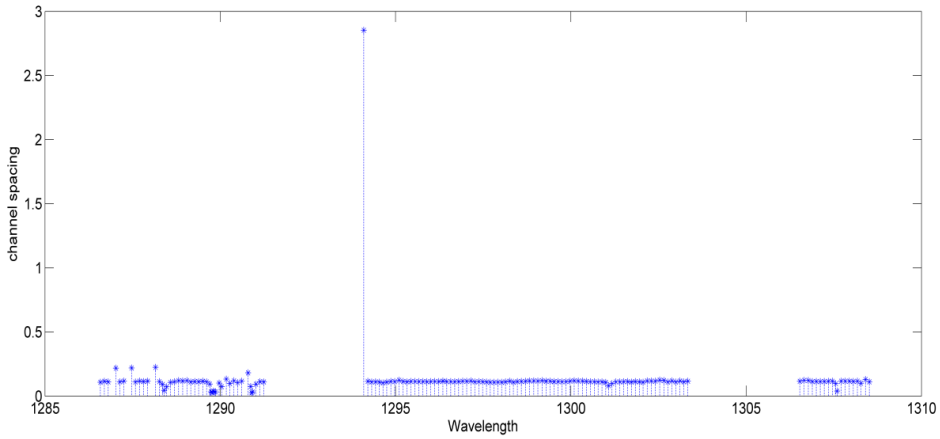

Figure 4.3.7: CW operation with 350 mA

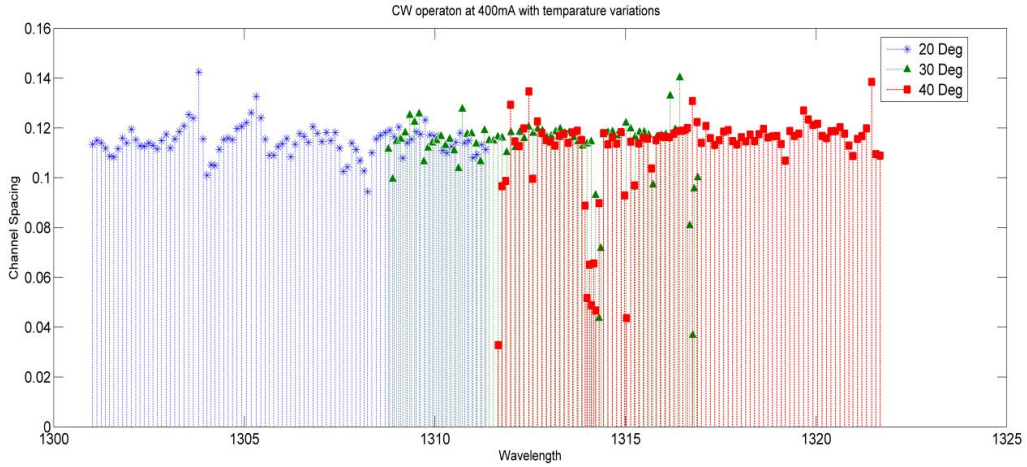

Figure 4.3.8: CW operation with 400 mA with temperature variation

Section Summary:

In the chapter, we briefly observed the 3-dB bandwidth (FWHM) dependability with different electrical injections as well as the stability for comb spectrums for the longer cavity.

REFERENCES

[1] Chi-Sen Lee, Wei Guo, Debashish Basu, and Pallab Bhattacharya, “High performance tunnel injection quantum dot comb laser "Appl. Phys. Lett. 96, 101107, 2010.
[2] Vivek Alwayn, Optical network design and implementation, Cisco press, 2004.
[3] Xu Peng-Fei et al, Chinese Phys. Lett. 28 044201, 2011.

CHAPTER 5

DISCUSSIONS

In this chapter, we discuss the previous findings observed from several performance trends. The overall findings for the tested high performance quantum dot comb laser can be summarized as follows:

- **Findings 1**: For this novel laser, threshold current density remains constant in spite of changes in the cavity length. However, there is a dominant effect of increased thermal conductivity in the smaller cavity when compared to the longer cavity. Additionally, the overall thermal conductivity due to static and dynamic heating caused by the injection current degrades the device performance of our Q.Dot comb laser.
- **Findings 2**: The novel emitter has a higher characteristic temperature than that of conventional semiconductor lasers which is around 50K. By increasing the external temperature, the performance of shorter cavity device drops drastically compared to the longer cavity ones.
- **Findings 3**: The overall full width half maximum (FWHM) bandwidth gets affected by increasing injection current. We also observed power drops with an increased current injection in the longer cavity devices; but in the shorter cavity devices, we have observed some dynamic nature with the increased injection due to the excited state lasing. Furthermore, we have observed better channel spacing stability with CW injection compared to the pulse injection. Finally, with cw injections, the channel spacing degrades at the higher temperatures due to an increased thermal effect.

The general findings provide the evidence of reduced thermal conductivity in Quantum Dot comb lasers with the increased temperature. The thermal effect is generated by an increased duty cycle or current. Moreover, additional thermal effects are produced by the resistive heating of the injection current, especially above the threshold. Thus, the laser behavior of quantum dot and quantum well is similar due to the combined heating effect [1]. In our experiment, the external differential quantum efficiency and slope efficiency decrease with the increase of duty cycle and with the elevated temperature. The decreasing slope efficiency indicates that the device performance degradation is temperature dependent [2]. Thus, it proves the existence of reduced thermal conductivity in the active layer for our quantum dot comb laser.

There are several possibilities which may contribute to performance deterioration such as increased auger recombination due to active layer p-doping, electron-hole scattering, large carrier leakage, intervalence band absorption, reservoir effects, and carrier distribution in dots as discussed in the literature. In the further discussions, we try to look into some of these possible factors that may affect the performance of our laser.

In our reported sample, the active layer of the comb laser is p-doped. This p-doping increases the temperature sensitivity at the price of increased threshold current, auger recombination and electron-hole scattering [3]. This doping level can affect the performance level in various ways. For example, such as Nelson et al. [4] reported that highly doped p-cladding can be used in the quantum well to suppress the carrier leakage

but may increase internal losses from $2cm^{-1}$ to 12 cm^{-1} through nonradioactive recombination. In the following section, we tried to observe the effect of internal loss due to change of duty cycle and temperature variance injection in our comb laser. The internal loss is analyzed from the relationship of external differential efficiency vs. cavity length.

Analysis of internal loss:

The p doping in the 8 layers of our quantum dot (Q.Dot) active region causes the performance degradation which can be verified from the following results. Taking x = 0.2 and effective index as 3.5 for the 1280 to 1300nm region, the calculated mirror loss is found to be: $\boldsymbol{\alpha}_m$ = 5.47 cm^{-1} for the shorter cavity (~ 1mm) and $\boldsymbol{\alpha}_m$ = 2.84 cm^{-1} for the longer cavity (~ 2mm). Thus, the internal loss is extracted from the slope of the $(1/\eta_d)$ versus the cavity length. These parameters can be extracted from the various cavity lengths such as 1mm, 1.4mm, 1.6mm, 1.8mm and 2mm etc. Since our measurements are done on 1mm and 2mm, it has been used to identify the trend of losses suffered due to the increasing duty cycle or temperature.

In figure 5.1, it's clearly depicted that internal loss approaches to mirror loss very fast for the shorter cavity and gradually for the longer cavity which causes more drastic performance degradation in the shorter cavity. Therefore, the short cavity laser has lower thermal conductivity compared to the longer cavity. In figure 5.2, we have also observed a similar phenomenon. While fixing the duty cycle at 1% and 20%, we have observed the drastic change in the internal loss. The loss increases if the resistive heating caused by

injection increases simultaneously. From figure 5.2, we can see that internal loss is increased at higher rates for 20% duty cycle pulse injection compared to that of 1%.

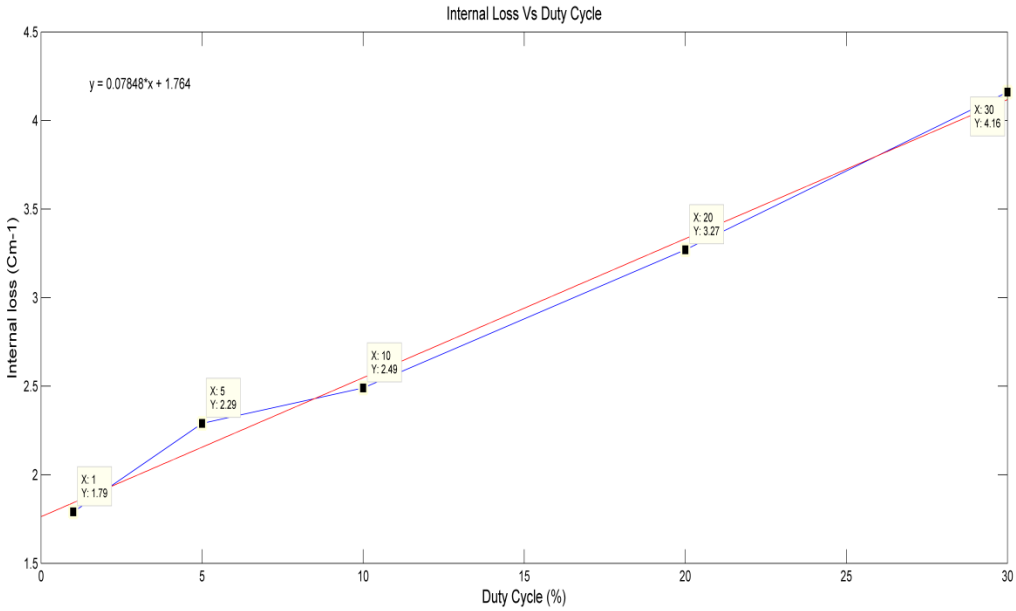

Figure 5.1: Change in internal loss with the duty cycle increment

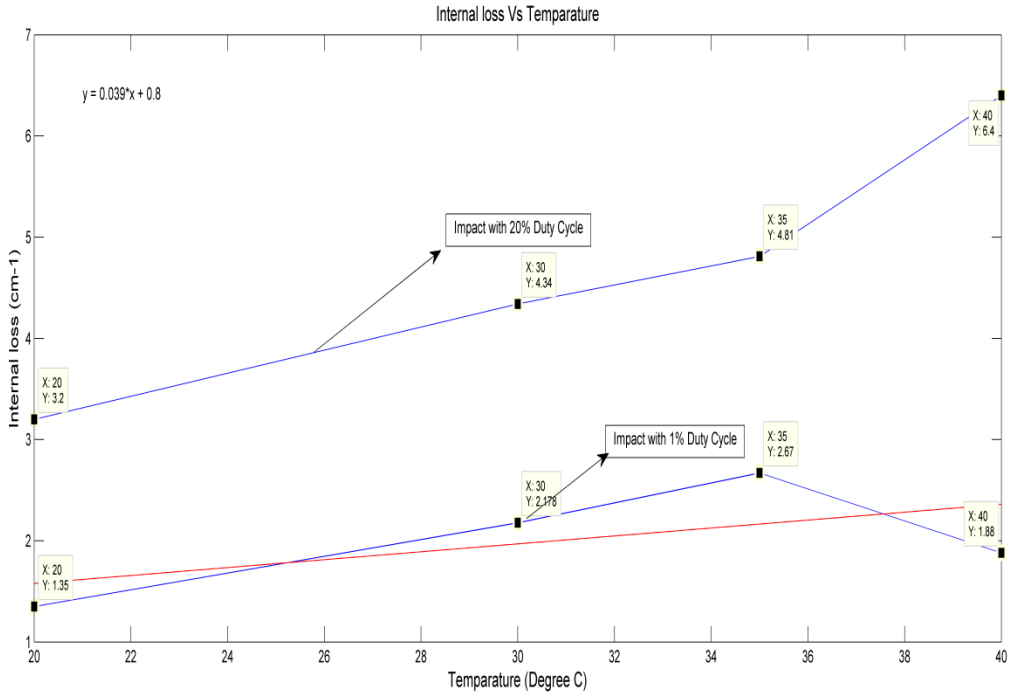

Figure 5.2: Change in internal loss with the variation of temperature

In the above figures, the red lines represent the linear fitted curve from the sampled points. Therefore, we can conclude that the internal loss is a dominating factor in the reduction of the slope efficiency. The internal losses may even approach the key mirror losses. The later sections, we will look into the factors that cause non-radiative recombination which is responsible for higher internal losses.

Contributing factors to the non-radiative recombination: In this part, we shall discuss a few non-radiative mechanisms which cause drop in slope efficiency. There are 3 main types of non-radiative recombination: auger-, defect-, and surface recombinations. But 1.3μm quantum dot lasers predominantly suffer from auger recombination as has been shown in several research studies [5].

Auger recombination: Auger recombination in III-V semiconductors is a combination of three processes: CCCH-, CHHS-, and CHHL- process and it is defined in equation 5.1 where C is the Auger coefficient, and n is the injected carrier density.

$$R = C \times N^3 \qquad (5.1)$$

The tested quantum dot comb laser suffers from increased auger recombination as the active layer has been doped with acceptors [3]. Even in the best InAs-GaAs based quantum dot lasers [6], there is always a presence of intrinsic auger recombination which accounts for 60% - 70% of J_{th} at room temperature (RT). Although p-type dopants are responsible for performance deterioration due to increased auger recombination, there are other certain facts to consider. In the following section, we will explain various pros and cons for employing p-doped active layers.

P-doping: P-dopants are important for increasing the temperature sensitivity of laser device because the practical data communication is moving towards higher bit rates. Therefore such devices are required to operate in ambient or uncooled environments (e.g. operating between -40^{o}C and 85^{o}C [7]). As a result, decreasing the temperature sensitivity for semiconductor lasers requires suitable material system and device structure to improve the characteristic temperature of the laser **[8]**. The characteristic temperature can be defined using the following formula,

$$I_{th} = I_0 \times e^{(T/To)} \qquad (5.2)$$

Equation 5.2 indicates that higher characteristic temperature T_o will lead to a lower threshold current and an increase in the temperature sensitivity of the device. Wang et al. [8] mentioned four factors affecting the characteristic temperatures: the active region bandgap, active region carrier leakage, auger recombination and intervalence band absorption. To improve the performance, a balance between these four factors is necessary. It is particularly obvious that auger recombination plays a vital role for the temperature sensitivity of the 1.3μm quantum dot lasers [9]. Hence, there are 2 primary methods that have been proposed to improve the characteristic temperature of 1.3-μm quantum dot lasers [10]: 1) Using multi-stacked quantum dot layers to increase the modal gain; 2) p-doping in the active region. It has been demonstrated that introducing p-dopants causes increased optical losses through increased non-radiative auger recombination as shown in figure 5.3.

Hence, there will be a tradeoff between introducing dopants or not, depending on the applications. P-doping reduces the temperature sensitivity at the cost of increased

nonradiative recombination at room temperature [11]. The best performed temperature independent 10Gb/s quantum dots laser uses p-doping and having characteristic temperatures above 400K as shown in the figure 5.4 [6, 12]. Clearly, increased auger recombination is detrimental consequence of introducing p-doping [**9**].

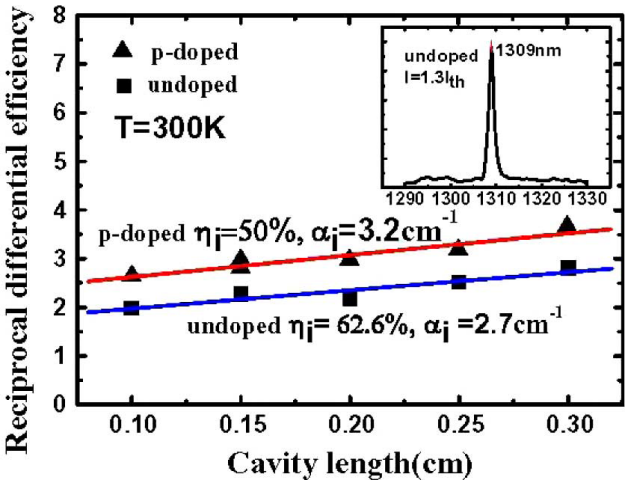

Figure 5.3: Comparison of doped and un-doped InAs-GaAs quantum dot laser [10]

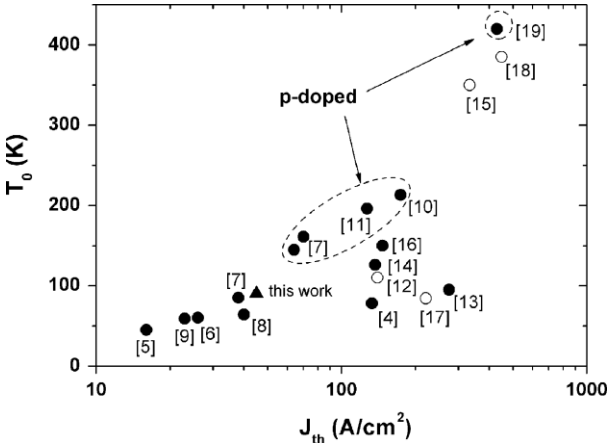

Figure 5.4: Comparison of characteristic temperature in 1.3-Quantum Dot laser [6]

Apart from that there might be other factors which may contribute to the performance deterioration as discussed in following sections, because increased auger recombination as a result of p-doping might not be the only factor. Gosh et al. [13] showed a striking

result for InGaAs/GaAs based quantum dot laser: a decrease in auger recombination occurred after an increase in temperature, this is believed to be caused by a temperature dependency of ground state hole occupation which controls the electron-hole scattering mechanism. Simultaneously, there are other possible probabilities responsible for performance degradations as described below:

Cavity length dependency: Cavity length analysis is important to understand the underlying reasons of the temperature sensitivity of quantum dot lasers. Shorter cavity lasers suffer from mirror loss due to the inverse relationship shown in equation 5.3 and plotted in figure 5.5 [9]. This also contributes to the increased threshold current density for the shorter cavity.

$$\alpha_m \propto \frac{1}{L} \qquad (5.3)$$

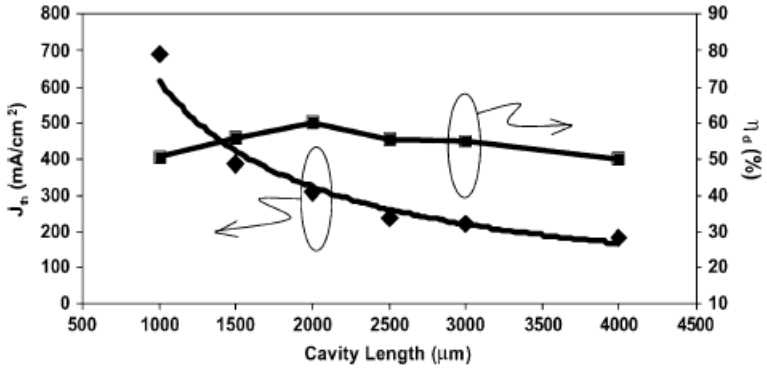

Figure 5.5: Cavity length effects on J_{th} and η_d [9]

Apart from the cavity lengths, excessive carrier exploitation in the active layer and carrier leakage may affect the performance of the device which will be elaborated in the subsequent sections.

Reservoir effect: As discussed previously, p-doping causes increased threshold current density in the device. Carrier capture processes in the quantum dot / wire / well lasers are not instantaneous and increasing the carrier density in the reservoirs leads to increased nonradiative recombination in the reservoir. This affects the lasers performance and limits the output power of the laser. Asryan et al. [14] argued that reducing the threshold current density is essential for the realization of high power quantum dot laser applications. The study also shows that quantum dot laser performance critically depends on the surface density of the quantum dots, size dispersion and cavity length. This is why p-doped devices might not be useful for high power laser applications since they must result in a high threshold current density.

Carrier leakage and escape: Above threshold, performance drops due to several thermal effects which make the trends of quantum dot lasers similar to those of quantum well lasers [1, 15]. The carrier leakage process is common for both the quantum dot / quantum well lasers [16] and this carrier leakage process is highly temperature sensitive [9]. In our experiment, we have observed a clear 10% decrease in the slope efficiency in some cases with increasing temperature. Such behavior can be attributed to carriers diffusing out from under ridge or carrier leakage as suggested [15].

In our high performance tunnel injection quantum dot laser, a tunneling barrier is used to confine the quantum dot and this carrier leakage can be reduced significantly [17] and allowing carriers to be transported to the lasing sub-band [18]. The tunneling

technique also improves the gain symmetry [19], which is important for the broad gain semiconductor laser.

High performance comb lasers are not only dependent on the internal structure of the quantum dots, the size dispersions and the cavity lengths but also on several other factors. Such factors include reduced auger recombinations, stacking required number of layers in the active layer, and adjusted p-doping level. Moreover, controlled injection using variable duty cycle rate is important to reduce the thermal effects for better stability of the device.

REFERENCES

[1] Tan, H.; Kamath, K.; Bhattacharya, R.; Klotzkin, D., "Evidence for reduced thermal conductivity in quantum dot active region from chirp characteristics in InGaAs/GaAs quantum dot lasers," Lasers and Electro-Optics Society, LEOS 2004. The 17th Annual Meeting of the IEEE , vol.2, no., pp. 619- 620 Vol.2, 7-11 Nov. 2004.

[2] G. Park, O. B. Shchekin, D. L. Huffaker and D. G. Deppe,"Low-threshold oxide-confined 1.3-μm quantum-dot laser", IEEE Photon. Techn. Lett. 12, 230–232 (March 2000).

[3] Chi-Sen Lee, Wei Guo, Debashish Basu, and Pallab Bhattacharya, "High performance tunnel injection quantum dot comb laser "Appl. Phys. Lett. 96, 101107, 2010.

[4] Tansu, N.; Ying-Lan Chang; Takeuchi, T.; Bour, D.P.; Corzine, S.W.; Tan, M.R.T.; Mawst, L.J.; ,"Temperature analysis and characteristics of highly strained InGaAs-GaAsP-GaAs ($\lambda > 1.17$ μm) quantum-well lasers," Quantum Electronics, IEEE Journal of , vol.38, no.6, pp.640-651, Jun 2002.

[5] Marko, I.P.; Andreev, A.D.; Adams, A.R.; Krebs, R.; Reithmaier, J.P.; Forchel, A.;, "Importance of Auger recombination in InAs 1.3 μm quantum dot lasers," Electronics Letters , vol.39, no.1, pp. 58- 59, 9 Jan. 2003.

[6] Marko, I.P.; Adams, A.R.; Sweeney, S.J.; Mowbray, D.J.; Skolnick, M.S.; Liu, H.Y.; Groom, K.M.; , "Recombination and loss mechanisms in low-threshold InAs-GaAs 1.3-μm quantum-dot lasers," Selected Topics in Quantum Electronics, IEEE Journal of , vol.11, no.5, pp. 1041- 1047, Sept.-Oct. 2005.

[7] T. Keating , X. Jin , S. L. Chuang and K. Hess,"Temperature dependence of electrical and optical modulation responses of quantum-well lasers", IEEE J. Quantum Electron., vol. 35, p.1526 , 1999.

[8] Yuxia Wang, Chunling Liu, Jilong Tang, Baoxue Bo, and Guojun Liu, "AlInGaAs/AlGaAs/GaAs strained quantum well lasers with high characteristic temperature," Chin. Opt. Lett. 5, S143-S144, 2007.

[9] N.-H. Kim; J.-H. Park; L.J. Mawst; T.F. Kuech; M. Kanskar;, "Temperature sensitivity of InGaAs quantum-dot lasers grown by MOCVD," Photonics Technology Letters, IEEE , vol.18, no.8, pp.989-991, April 2006.

[10] Yulian Cao, Tao Yang, Haiming Ji, Wenquan Ma, Qing Cao, Lianghui Chen, "Temperature Sensitivity Dependence on Cavity Length in p-Type Doped and Undoped 1.3-μm InAs–GaAs Quantum-Dot Lasers", Photonics Technology Letters, IEEE, On page(s): 1860 - 1862, Volume: 20 Issue: 22, Nov.15, 2008

[11] Smowton, P.M.; Sandall, I.C.; Mowbray, D.J.; Hui Yun Liu; Hopkinson, M.;, "Temperature-Dependent Gain and Threshold in P-Doped Quantum Dot Lasers," Selected Topics in Quantum Electronics, IEEE Journal of , vol.13, no.5, pp.1261-1266, Sept.-oct. 2007.

[12] N. Hatori, K. Otsubo, M. Ishida, T. Akiyama, Y. Nakata, H. Ebe, S. Okumura, T. Yamamoto, M. Sugawara, and Y. Arakawa, "20◦C–70◦C temperature independent 10 Gb/s operation of a directly modulatedlaser diode using P-doped quantum dots," presented at the 30th Eur. Conf. Optical Communication, Stockholm, Sweden, Sep.2004, Postdeadline paper.

[13] Ghosh S, Bhattacharya P, Stoner E, Singh J, Jiang H, Nuttinck S and Laskar J, "Temperature-dependent measurement of Auger recombination in self-organized $In_{0.4}Ga_{0.6}As/GaAs$ quantum dots", Appl. Phys. Lett. 79 722-4, 2001.

[14] Asryan, L.V.; Luryi, S.; Suris, R.A.;, "Internal efficiency of semiconductor lasers with a quantum-confined active region," Quantum Electronics, IEEE Journal of , vol.39, no.3, pp. 404-418, Mar 2003.

[15] David Klotzkin and Pallab Bhattacharya, "Temperature Dependence of Dynamic and DC Characteristics of Quantum-Well and Quantum-Dot Lasers: A Comparative Study," J. Lightwave Technol. 17, 1634-, 1999.

[16] J. Piprek, P. Abraham, and J. E. Bowers, "Cavity length effects on internal loss and quantum efficiency of multi-quantum-well lasers", IEEE J. Select. Topics Quantum Electron., vol. 5, pp.643 - 647 , 1999.

[17] Z. Mi, P. Bhattacharya, and S. Fathpour, "High-speed 1.3 μm tunnel injection quantum-dot lasers", Appl. Phys. Lett., vol. 86, p. 153109, Apr. 2005.

[18] Dutta, Mitra, and Michael A. Stroscio, Advances in Semiconductor Lasers and Applications to Optoelectronics. Singapore: World Scientific, 2000.

[19] Hua Tan; Zetian Mi; Bhattacharya, P.; Klotzkin, D.;, "Dependence of Linewidth Enhancement Factor on Duty Cycle in InGaAs–GaAs Quantum-Dot Lasers," Photonics Technology Letters, IEEE , vol.20, no.8, pp.593-595, April15, 2008.

CHAPTER 6

CONCLUSIONS AND RECOMMENDATIONS

The high performance comb laser is found to be one of the salient emitters for next generation short reach interconnects. However, thorough device level characterization is required in order to improve the performance level for real system implementation. Therefore, we demonstrated several performance trends of the device which has been tested by varying the temperature, duty cycle and cavity length. We have also studied the impact of temperature and injection on overall bandwidth and spectrum stability of the comb laser.

From the findings, it's clear that device performance is strongly affected by the temperature and the injection induced heating effect which proves the lower thermal conductivity of the active layer of the quantum dot laser. Similar trends have been observed in the literature for 1.3-μm quantum dot lasers.

We reported that the main factor for decreasing overall efficiency is increased internal losses in the active layer which results from the increased electrical pumping and temperature level. Although carrier leakage has been reduced in such lasers with the tunnel injection mechanism, there is strong evidence of auger recombination due to the p-doping. Furthermore, p-doping is necessary for increasing the temperature sensitivity of the lasers which is necessary for high bit rate computer communications. Thus, it is essential to reduce active layer thermal effects, auger recombination, and temperature induced internal losses while maintaining uniform gain with sufficient power to achieve

the required performance level. Such a comb laser would be a very attractive choice in optical transceiver systems and a cost-effective solution for converging WDM-PON and short-reach interconnects.

For future work, there are several other factors that influence laser performance which need to be studied. Such factors include the study of stability for the individual spectrum through temperature and injection variation, the level of cross-talk between the channels and relative intensity noise (RIN) for the individual channel, and the testing of small signal and large signal modulation bandwidth to support high scale date transfer rate. Furthermore, to improve thermal conductivity of high performance quantum dot comb laser; identifying the effects of auger recombination, p-doping, electron-hole scattering, and carrier leakage is necessary.